


Review

# Electrochemical Sandwich Assays for Biomarkers Incorporating Aptamers, Antibodies and Nanomaterials for Detection of Specific Protein Biomarkers

Dharmendra Neupane and Keith J. Stine \* 

Department of Chemistry and Biochemistry, University of Missouri, Saint Louis, MO 63121, USA; dnzf@mail.umsl.edu

\* Correspondence: kstine@umsl.edu; Tel.: +1-314-516-5346

**Abstract:** The development of sensitive and selective assays for protein biomarkers and other biological analytes is important for advancing the fields of clinical diagnostics and bioanalytical chemistry. The potential advantages of using aptamers in electrochemical sandwich assays are being increasingly recognized. These assays may include an aptamer as both capture and detection agent or a combination of an aptamer with a different partner such as an antibody, a lectin or a nanomaterial. The second binding partner in the sandwich structure is typically conjugated to a redox marker, a catalyst or an enzyme that can be used to generate the signal needed for electrochemical detection. Nanoparticles and other nanostructures can be used as the carriers for multiple molecules of the detection partner and thereby increase the signal. Nanostructured surfaces can be used to increase surface area and improve electron transfer. Sensitive electrochemical methods including impedance, differential and square-wave voltammetry and chronocoulometry have been used for electrochemical signal read-out. Impressive results have been achieved using electrochemical sandwich assays in terms of limit of detection and linear range for a growing range of analytes. The recent progress for this type of assay for proteins and other biomarkers is the subject of this review.

**Keywords:** assay; sandwich assay; aptamer; protein; electrochemistry; biomarker



**Citation:** Neupane, D.; Stine, K.J. Electrochemical Sandwich Assays for Biomarkers Incorporating Aptamers, Antibodies and Nanomaterials for Detection of Specific Protein Biomarkers. *Appl. Sci.* **2021**, *11*, 7087. <https://doi.org/10.3390/app11157087>

Academic Editor:  
Chris Papadopoulos

Received: 11 June 2021  
Accepted: 28 July 2021  
Published: 31 July 2021

**Publisher's Note:** MDPI stays neutral with regard to jurisdictional claims in published maps and institutional affiliations.



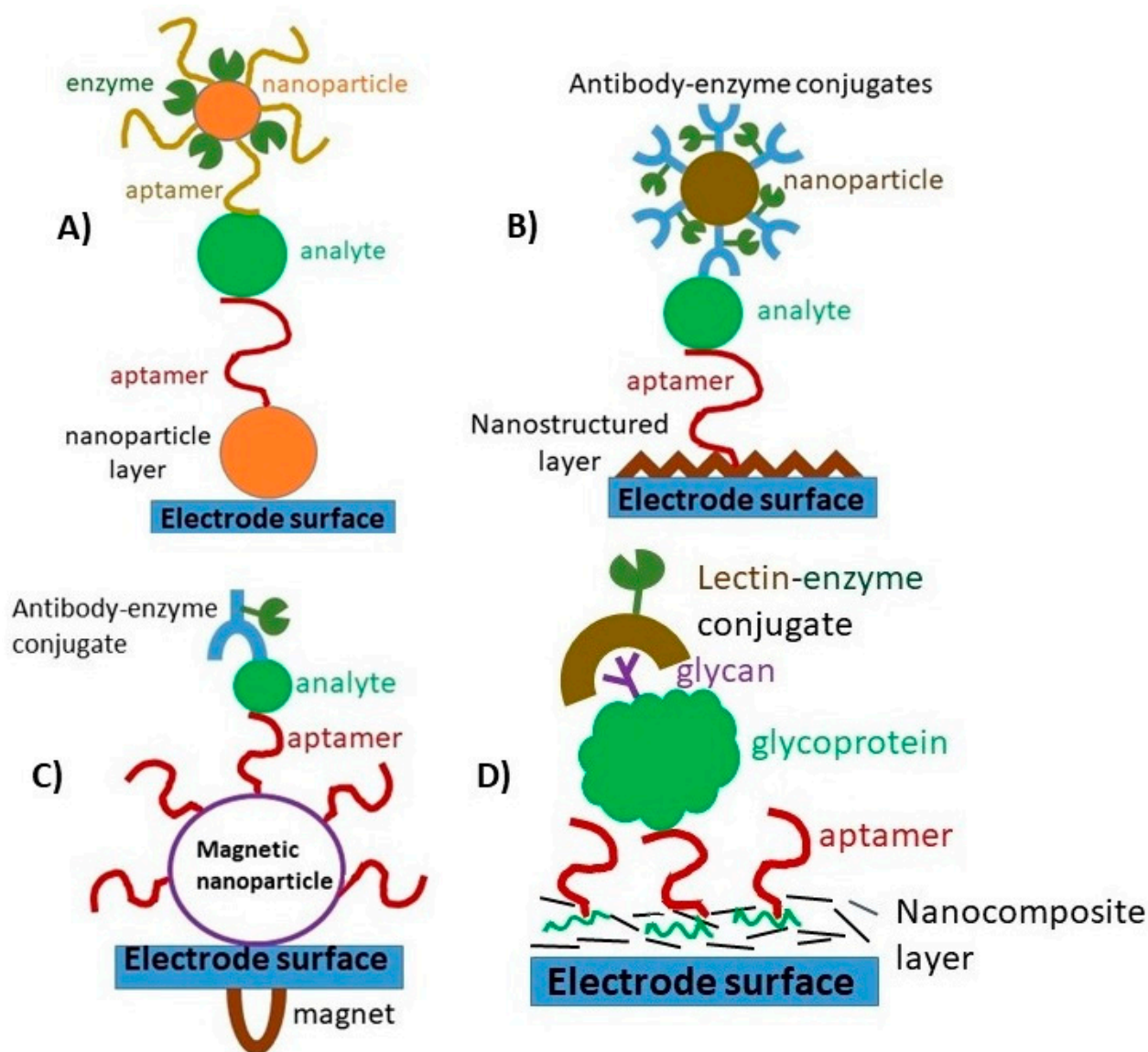
**Copyright:** © 2021 by the authors. Licensee MDPI, Basel, Switzerland. This article is an open access article distributed under the terms and conditions of the Creative Commons Attribution (CC BY) license (<https://creativecommons.org/licenses/by/4.0/>).

## 1. Introduction

As a strategy for increasing sensitivity and selectivity, the development of electrochemical assays using aptamers in sandwich structures has become popular. In these assays, the analyte is sandwiched between two aptamers, between an aptamer and an antibody, or between an aptamer and another agent such as a lectin or a nanomaterial. In all of these approaches, the incorporation of nanostructured surfaces and nanoparticles or nanomaterials of many kinds has been pursued to enhance the electrochemical signal and improve the limits of detection and selectivity. In the past five years, the range of analytes studied has broadened to include more protein biomarkers of diagnostic significance. Additionally, in this period, the range of nanomaterials and nanostructures incorporated both on electrode surfaces and as labels for detection agents has grown in the past 5 years to include nanowires, metal–organic frameworks, nanosheets and templated natural nanostructures. Scheme 1 shows a selection of the sandwich assay architectures described in this review and some of the kinds of surfaces on which these assays have been performed and demonstrates the breadth of possibilities.

The most studied analyte for electrochemical sandwich assays involving aptamers is the serine protease thrombin, so in this review, we first profile sandwich assays for this analyte as a major example of the growing diversity of assay architectures. We then review electrochemical assays for other analytes that use two aptamers in the sandwich, assays that combine an aptamer and an antibody, and assays that combine an aptamer with a lectin or a nanomaterial as the second partner in the structure. The broader role

of aptamer-based electrochemical sensors in medical diagnostics is reviewed including strategies based on hybridization and changes in aptamer conformation [1]. An interesting earlier review concerning electrochemical sandwich assays is also presented [2]. The most common electrochemical detection strategies are those that detect a peak current and those that detect an accumulation of charge by binding a redox marker to the surface-bound oligonucleotides associated with the detection part of the sandwich structure.



**Scheme 1.** A sample of some of the sandwich assay structures that are possible and that are discussed in this review. (A) an aptamer–analyte–aptamer sandwich with capture aptamers bound to a nanoparticle-modified electrode surface with the detection aptamers bound to a nanoparticle that also is labeled by an enzyme, (B) an aptamer–analyte–antibody sandwich on a nanostructured layer which has continuous nanoscale features to which capture aptamers are bound with the detection antibodies then bound to a nanoparticle in the form of antibody–enzyme conjugates, (C) aptamer-modified magnetic nanoparticles captured on an electrode surface using a magnet so that an aptamer–analyte–(antibody–enzyme conjugate) sandwich structure can be formed, and (D) a nanocomposite surface containing materials such as carbon nanotubes and polymers with adsorbed or covalently attached aptamers forming a sandwich with a glycoprotein for which the glycan structure is bound by a lectin–enzyme conjugate. There are numerous other possibilities. The linkage of aptamers to surfaces or nanoparticles may be by the use of thiolated aptamers, the use of bioconjugation reactions, biotin–streptavidin interactions or by physisorption. Enzymes may be linked to aptamers or antibodies using biotin–streptavidin interactions, or bioconjugation reactions. The analyte is most often a protein biomarker but can also represent other possibilities such as a cell, a bacterium, a peptide, or some other biomolecule.

Electrochemical approaches to detecting biomarkers for a wide range of diseases are under intensive development focusing on specific proteins, peptides, and oligonucleotides [3]. Electrochemical detection of specific protein biomarkers is a key technology under development for the diagnosis of cancer and other diseases in clinical and point-of-care settings [4]. Electrochemical immunosensors based on antibodies and antibody sandwich complexes have become a highly popular approach [5–7]. Electrochemical assays have the advantage of making use of low-cost instrumentation, ease of implementation, and offer good prospects for high sensitivity and selectivity. Electrochemical assays can be developed for a very wide range of biomarkers by using the appropriate recognition molecules and designing an assay resulting in a current or charge response that is related to biomarker concentration. As an alternative to antibodies, aptamers possess several appealing features for application in biosensors, such as their stability, high specificity and sensitivity, ease of re-use and small size compared to other agents such as antibodies [8]. Whereas antibody probes can be subject to irreversible denaturation, aptamers can be reliably regenerated.

The desired aptamer is developed using the systematic evolution of ligands by the exponential enrichment (SELEX) process. SELEX starts with an initial library of oligonucleotides and through a number of cycles identifies an oligonucleotide that has a strong affinity for the target. The oligonucleotides in the initial pool consist of a random internal region of base pairs and constant flanking regions of typically 15 to 20 base pairs long needed for the polymerase chain reaction (PCR) amplification step [9]. A random region of 20 base pairs would present the possibility for  $4^{20} = 1.1 \times 10^{12}$  possible sequences. The number of nucleotides in the random region can be as high as 60. The initial pool does not contain all of the possibilities, especially for longer lengths of the random region [10]. A SELEX cycle consists of allowing the target to bind to oligonucleotides in the pool, followed by a selection of those that have bound to the target, and their amplification in advance of the next cycle. A typical process when the target is a protein involves allowing the protein to mix with the oligonucleotide pool in solution so that the sequences with higher affinities can bind to the protein. Nitrocellulose membranes are frequently used to capture the oligonucleotide–protein complexes and pass through the free oligonucleotides [11]. The proteins can also be captured on activated sepharose and the unbound oligonucleotides removed [12]. The oligonucleotides sequences that are bound to the captured proteins are released so that they can be subjected to amplification [13]. While aptamers are identified from pools of ssDNA oligonucleotides, aptamers based on RNA are also known [14]. There have been many variations in the SELEX process reported [15]. The affinities achieved for protein targets using aptamers are as high as those achieved by most antibodies, and are in the 1–100 nM range [10].

In their use as capture agents on gold electrode surfaces, or for example, as reporter agents on gold nanoparticles, aptamers with thiolated ends can readily be prepared. Aptamers designed for immobilization on gold typically have a linker such as a short alkyl chain attached to one end of the oligonucleotide and a disulfide with mercaptohexanol on the other end [16]. Reduction with dithiothreitol or with tris(2-carboxyethyl)phosphine (TCEP) is used to produce the free thiol. The disulfide form can directly modify a gold surface but will result in lower aptamer surface density. Derivatives of the 15-mer and 29-mer aptamers against thrombin have been reported in which the 5'-end was modified with two dithianes with a phosphodiester bridge and a short polyethylene glycol (PEG) linker resulting in especially strong and flexible binding to the gold surface [17]. When carbon-based electrodes are used, a strategy for aptamer immobilization is to generate carboxyl groups on the surface and conjugate amine-terminated aptamers using EDC/NHS chemistry [18]. Immobilization of aptamers on glassy carbon electrodes has also been achieved using  $\pi$ -stacking on a spread graphene–porphyrin composite [19]. The adsorption of a graphene/apptamer complex onto glassy carbon electrodes modified by poly(o-phenylenediamine) has been reported [20]. Pyrene units at the 3'-end were used for aptamer immobilization onto reduced graphene oxide [21]. It is also possible to covalently

attach aptamers to carbon electrodes using diazonium salt chemistry [22]. Methods for immobilization of aptamers onto surfaces are reviewed [23].

Given these advantageous properties, significant efforts have been pursued in recent years for the development of biosensors for proteins and some small molecules using aptamers and electrochemical detection strategies have been a prime focus. The need for protein biosensors is strongly driven by the desire to detect proteins that serve as biomarkers for various disease states in clinical and diagnostic settings. If there are two different aptamers available that bind to different sites on a protein, then one aptamer can be immobilized on an electrode surface to serve as the capture aptamer, and another can then serve as the reporter aptamer and bind from the solution to another site on the protein. If only one aptamer binding to one site on the target protein is available, then an antibody partner can be employed that binds to another site either in the capture or reporter role. The nature of the electrode surface can also be varied, using simple flat gold films or glassy carbon, or more elaborate nanostructured surfaces whose higher surface area can also contribute to signal amplification. While gold electrodes are widely used, other types of electrodes such as glassy carbon have also been regularly employed. Aptamer-based systems for these electrochemical assays are steadily emerging and show great potential as described in this review.

## 2. Electrochemical Sandwich Assays for Thrombin Using Aptamers

Thrombin, which is a serine protease present in the blood during ongoing coagulation, serves as a biomarker for diseases including Alzheimer's [24] and cancer [25]. Thrombin is by far the most studied analyte in electrochemical sandwich assays using aptamers because two complimentary thrombin binding aptamers have been developed. A 15-mer aptamer was first discovered [26] and later a 29-mer [27], each binding to different sites of the protein. The 15-mer forms a G quadruplex that interacts with the fibrinogen recognition exosite by mainly electrostatic interactions [28] and has a reported  $K_d$  value of  $\sim 100$  nM. The 29-mer aptamer binds to the heparin-binding exosite of thrombin with hydrophobic interactions and duplex formation being significant and resulting in  $K_d = 0.5$  nM [29]. These two sites on the protein are well separated.

Numerous approaches have been reported for the detection of thrombin using aptamers, including optical, electrochemical and chromatographic affinity-based assays [30]. Thrombin can be an important biomarker for diseases that involve changes or abnormalities in the coagulation process [31]. Thrombin is an important component of the coagulation cascade [32]. Thrombin is a serine protease homologous to other serine proteases such as chymotrypsin [33]. The precursor to thrombin, prothrombin, circulates in the blood at a concentration of  $1.4 \mu\text{M}$ . The relevant physiological range of thrombin concentration is low nanomolar to low micromolar [34]. The appeal of thrombin as a target, as noted above, is that there are two aptamers available that target two different, spatially separated sites on the protein making formation of a sandwich structure readily achieved. Some electrochemical assays have made use of only one aptamer, such as an assay based on aptamer conformational change upon thrombin binding [35]. A 32-mer aptamer for thrombin would undergo a conformational change from unfolded to G-quartet conformation that binds to thrombin. The distance of a redox label, methylene blue conjugated to the 3'-end, from a gold electrode surface increased upon thrombin binding. The peak current in a differential pulse voltammetry sweep would decrease with increasing thrombin concentration. Analysis using the Laviron equation [35] revealed that binding of thrombin reduced the kinetic rate constant from  $88 \text{ s}^{-1}$  to  $58 \text{ s}^{-1}$ , attributed to a change in the electron transfer pathway due to a binding-induced conformational change. A linear response for thrombin spiked in fetal calf serum was seen from  $6.4$ – $768$  nM. Other methods aside from Electrochemistry used to detect thrombin using aptamers have included a guided-mode resonance (GMR) sensor [36] which is an optical method based on the change in refractive index showing up as a shift in transmittance of a grating structure. The  $\text{SiO}_2$  on the GMR sensor surface was modified with 3-aminopropyltriethoxysilane and then conjugated to the 29-mer for



thrombin, which is the one of higher binding affinity. This sensor achieved a detection limit of 0.19  $\mu\text{M}$  and a linear range of 0.25–1.0  $\mu\text{M}$ . Using a Biacore SPR chip, a multiple sandwich assay for thrombin was reported that achieved a detection limit of 0.1 aM (attomolar), and a range from 0.1–4.0 aM [37]. In this approach, a gold sensor chip was first modified with a mixture of mercaptoundecanoic acid and a PEGylated alkanethiol followed by conjugation of an anti-thrombin antibody using EDC/NHS chemistry. The thrombin bound to the antibody was then exposed to the 29-mer binding sequence thrombin aptamer but with a polyadenine tail of 30 units in length. The SPR response was enhanced using a dual nanoparticle strategy, where gold nanorods (length =  $50 \pm 10$  nm, width =  $10 \pm 2$  nm) modified by poly(thymine) chains of 20 units would then bind to roughly spherical gold nanoparticles ( $50 \pm 5$  nm) modified by poly(adenine) chains of 30 units.

An early report made use of electrochemical impedance spectroscopy (EIS) as the detection method for an assay and used the increase in charge transfer resistance ( $R_{ct}$ ) as the response versus thrombin concentration [38]. In the assay, a gold electrode was modified by thiolated 15-mer aptamer (5'-HS-(CH<sub>2</sub>)<sub>6</sub>-GGTTGGTGTGGTTGG-3') and mercaptohexanol or mercaptoethanol were used to fill in bare spots on the electrode surface. The use of mercaptoethanol was found to be preferred as it gave the best response in EIS. Incubation with thrombin solutions of varying concentrations took place for 60 min. A sandwich structure was then formed by incubation with aptamer-modified gold nanoparticles that had their surface filled in by rhodamine-6G which presumably interacts with the nanoparticle surfaces through its two N-H groups. The gold nanoparticles modified by DNA are negatively charged and thus repel the [Fe(CN)<sub>6</sub>]<sup>3-/4-</sup> probes used in the buffer for conducting impedance spectroscopy. In this work, the same aptamer was used on the surface and on the nanoparticles. The ratio of  $R_{ct}$  for thrombin solution to  $R_{ct}$  of a blank solution was plotted versus thrombin concentration and a detection limit of 0.02 nM was achieved with a linear range from 0.05–18 nM. BSA used as a control showed a minimal response. The presence of the adsorbed rhodamine 6G was found to increase the response and was also noted as of potential use as a Raman probe for detection of thrombin binding using surface-enhanced Raman spectroscopy (SERS). Two different anti-thrombin aptamers that recognized different binding sites of the targeted thrombin were assembled on the surface of the gold electrode for the fabrication of the electrochemical sensor system [39]. Glucose dehydrogenase (GDH) from *Burkholderia cepacia* was used as the label on the detecting aptamer. The two different aptamers were the 15-mer aptamer, 5'-GGTTGGTGTGGTTGG-3' and the other was a 29-mer aptamer, 5'-AGTCCGTGGTAGGGCAGGTTGGGGTGA-3' with  $K_d$  values of 26 nM and 0.5 nM, respectively. The thiolated aptamer (29-mer) was immobilized on the surface of the gold electrode followed by the target thrombin and the GDH labeled (15-mer) second aptamer. BSA was used as the control protein. The lower limit of the detection of this system was 1  $\mu\text{M}$ . In a thrombin detection study using potentiometric detection, gold electrodes were first modified by a thiolated primary aptamer and filled in with 6-mercaptohexanol [40]. After binding with thrombin for 1 h, the bound thrombin was exposed to CdS quantum dots modified by the secondary aptamer. The CdS quantum dots were oxidized for 15 min using 0.01 M H<sub>2</sub>O<sub>2</sub> and then the Cd<sup>2+</sup> ions were detected using a solid-contact ion-selective microelectrode. The EMF vs. log(thrombin, ppm) was nearly linear and useful for detection over a range of 10–250 ppb with a detection limit of 5 ppb (0.14 nM). Another impedimetric study made use of Au nanoparticle-modified sheets of reduced graphene oxide (rGO) to provide amplification of the charge transfer resistance response to formation of the capture aptamer–thrombin–reporter aptamer sandwich [41]. Gold electrodes were modified with thiolated capture aptamer and filled with dithiothreitol. In a one-pot reaction, rGO was generated from graphene oxide and decorated with 7.5 nm Au nanoparticles. The thiolated reporter aptamer was bound to these gold nanoparticles. Incubation with thrombin was done for 90 min and the incubation with the rGO-Au nanoparticle conjugates required 5 h to reach saturation. The increase in charge transfer resistance to thrombin concentration was linear from 0.3–50 nM with a detection limit of 0.01 nM.

In addition to flat gold surfaces, electrodes with nanostructured surfaces or assemblies of gold nanoparticles have been used to enhance surface area as an additional means to achieve signal amplification. An aptamer sandwich assay on nanoporous gold (NPG) electrode was used to achieve high sensitivity with chronocoulometric detection for detection of thrombin [42]. An electrode of high surface area was created by generating a nanoporous gold layer by applying a square wave potential pulse to a gold disc electrode in a highly basic solution (2 M NaOH). The roughness factor of this electrode as determined using oxide stripping in cyclic voltammetry was ~34. The NPG electrode was first modified by thiolated 15-mer aptamer with a TTTTT tail (5'-SH-(CH<sub>2</sub>)<sub>6</sub>-TTTTT-GTTG-GTGTG-GTTGG-3') and then mercaptohexanol was allowed to assemble to fill in bare spots and provide better orientation of the aptamers. Subsequent or co-addition of mercaptohexanol for self-assembly of oligonucleotides onto Au is an established strategy for providing better orientation and filling in bare spots between aptamers on a gold surface [43]. Aptamer-modified gold nanoparticles of 3.2 nm diameter were prepared modified by a 3/1 ratio of non-binding aptamer to binding aptamer with the goal of having each modified nanoparticle bind to only one thrombin. Electrochemical impedance spectroscopy was used to characterize the extent of surface modification after each step in electrode modification and sandwich formation through the increase in charge transfer resistance. The detection step used the electrostatic binding of [Ru(NH<sub>3</sub>)<sub>6</sub>]<sup>3+</sup> to the DNA strands in the outer regions of the sandwich complexes. The binding of greater numbers of aptamer-modified Au nanoparticles to the thrombin captured on the aptamer-modified electrode resulted in the accumulation of a greater amount of [Ru(NH<sub>3</sub>)<sub>6</sub>]<sup>3+</sup> which was then detected by the amount of charge passed as measured by chronocoulometry upon reduction of [Ru(NH<sub>3</sub>)<sub>6</sub>]<sup>3+</sup> to [Ru(NH<sub>3</sub>)<sub>6</sub>]<sup>2+</sup>. The difference in charge passed in the presence and absence of thrombin was plotted versus thrombin concentration achieving a detection limit of 30 fM and a linear range from 0.01–22 nM. The selectivity of the biosensor was tested using fibrinogen, prothrombin, and Factor Xa and found to be excellent. The times required for incubation with thrombin and then with the aptamer-modified nanoparticles were reported each as 2 h.

An approach using magnetic beads was used to perform an aptamer-based electrochemical sandwich assay for thrombin [44]. Streptavidin-coated magnetic beads were first used to bind the biotinylated 15-mer aptamer (primary aptamer) followed by binding of thrombin and then binding of biotinylated 29-mer aptamer (secondary aptamer). Optimization of conditions resulted in the choice of 0.1 μM 29-mer biotinylated aptamer and an incubation time of 15 min. Incubation with thrombin was also for 15 min. Incubation with streptavidin–enzyme conjugate was carried out for 10 min. Each step was performed in an appropriate buffer. The bound sandwich complexes were then attracted to a screen-printed carbon electrode. The amount of thrombin bound was then assayed by measuring the current peak due to reduction of the 1-naphthol product obtained by the action of the alkaline phosphatase enzyme on the substrate 1-naphthyl phosphate. A nonlinear dose–response curve was observed. A detection limit of 0.45 nM was obtained, and the assay was useful over the range 0.1–100 nM. Selectivity in the presence of 72 μM human serum albumin was only slightly greater than that obtained using buffer alone as a blank. The response for thrombin spiked into 10× diluted serum was similar to that obtained in the buffer.

Assays for thrombin using magnetic beads were reported in indirect competitive, direct competitive and product detection formats [45]. In the indirect competitive assay, thrombin conjugated to magnetic beads competed with free thrombin for binding of biotinylated 15-mer aptamer. Subsequently, the biotinylated aptamer captured on the magnetic beads could bind to alkaline phosphatase labeled streptavidin. In the direct competitive assay, 15-mer aptamer-modified magnetic beads competed to bind thrombin from solution in the presence of biotinylated thrombin and then alkaline phosphatase labeled streptavidin was bound onto the captured thrombin. The magnetic beads were then captured on the electrode surface by a magnetic field, washed, and the activity of alkaline phosphatase for the substrate 1-naphthyl phosphate was measured by differential pulse

voltammetry detection of the 1-naphthol product. The direct competitive assay achieved a detection limit of 430 nM. The indirect competitive assay was subject to too much non-specific adsorption of the alkaline phosphatase labeled streptavidin to be useful as an assay. The enzymatic activity of thrombin captured onto aptamer-modified magnetic beads was assayed using the substrate  $\beta$ -Ala-Gly-Arg-p-nitroaniline by detection of the released p-nitroaniline by its reduction peak using DPV. A detection limit of 175 nM was achieved using this approach. This study confirmed that the detection limit of 0.45 nM achieved using the sandwich assay approach [45] was superior, and additionally, the sandwich assay displayed outstanding selectivity in the presence of 72  $\mu$ M human serum albumin.

A novel electrochemical biosensor based on the aptamer and the signal amplification by gold nanoparticles was fabricated for the determination of thrombin [46], as shown in Figure 1. The aptamer was immobilized on the Au NPs coated gold electrode for about 16 h followed by 6-mercapto-1-hexanol for about 1 h to block the uncovered parts of the surface. The aptamer-modified electrode then interacted with different concentrations of the thrombin followed by incubation in the solution contain AuNP probes. AuNP probes were prepared by incubating 25 nm Au particles in the solution containing the aptamer and CdS-ssDNA for 16 h with gentle shaking. The resulting sandwich complex was treated with 1.0 M HNO<sub>3</sub> to dissolve the CdS nanoparticles. DPV measurements of the dissolved Cd<sup>2+</sup> were performed to measure anodic stripping peak currents. Thrombin was detected in this assay in the linear range of 1.0 fM to 10 pM with the detection limit of 0.55 fM of the target protein. Detection of the thrombin was done by an aptasensor with platinum nanoparticles (PtNPs) decorated carbon nanocages (CNCs) as signal labels [47]. PtNPs of 3–5 nm in diameter were dispersed on the surface of CNCs. The thiolated aptamer was immobilized on the surface of the gold electrode to capture the thrombin, and then aptamer functionalized PtNPs/CNCs nanocomposites were used to fabricate a sandwich aptasensor. The aptasensor was tested by recording the electrocatalytic reduction current toward H<sub>2</sub>O<sub>2</sub> by CV, EIS and DPV. The thrombin probe used was 5'-SH-(CH<sub>2</sub>)<sub>6</sub>GGTTGGTGTGGGTTGG-3'. The linear response of the aptasensor ranged from 0.05 pM to 20 nM with a low limit of detection of 10 fM. The aptasensor provided excellent specificity toward thrombin in the mixture of other proteins including BSA, Hb, L-vys, lysozyme, and spiking of thrombin with different concentrations into the 10-fold diluted serum.

Graphene doped with sulfur and nitrogen has improved electrical conductivity and was combined with gold nanoparticles and two aptamers to produce a highly sensitive electrochemical sandwich assay for thrombin [48]. One of the thrombin aptamers was thiolated on the 5'-end with a poly(T) tail (5'-SH-(CH<sub>2</sub>)<sub>6</sub>-TTTTTTTTTTGGTTGGTGTGGTTGG-3'). A glassy carbon electrode was modified by casting the doped graphene oxide dispersed with Au nanoparticles and then modifying it with the thiolated aptamer. A second dispersion was prepared of doped graphene oxide-modified with gold nanoparticles and then modified with an aptamer both thiolated on the 3'-end and biotinylated on the 5'-end (5'-biotin-AGTAGGCGGCGTTATGGTATTTTTTTTTTTTTTTT-SH-3'). Incubation with thrombin in phosphate buffer was carried out for one hour at 37 °C and then after washing exposure to the dispersion of aptamer-modified gold nanoparticles on doped graphene oxide took place for 80 min. The biotinylated aptamer was then bound to horseradish peroxidase-labeled avidin. Electrochemical detection of the oxidation of hydroquinone by H<sub>2</sub>O<sub>2</sub> by DPV was used as the response to increasing thrombin concentration. The detection limit achieved in phosphate buffer was 25 fM and a linear range of response was found from 100 fM to 10 nM. Selectivity was excellent when tested against human serum albumin,  $\alpha$ -fetoprotein, and carcinoembryonic antigen. Agreement between thrombin spiked into human serum samples from 50 fM to 50 pM was very good.

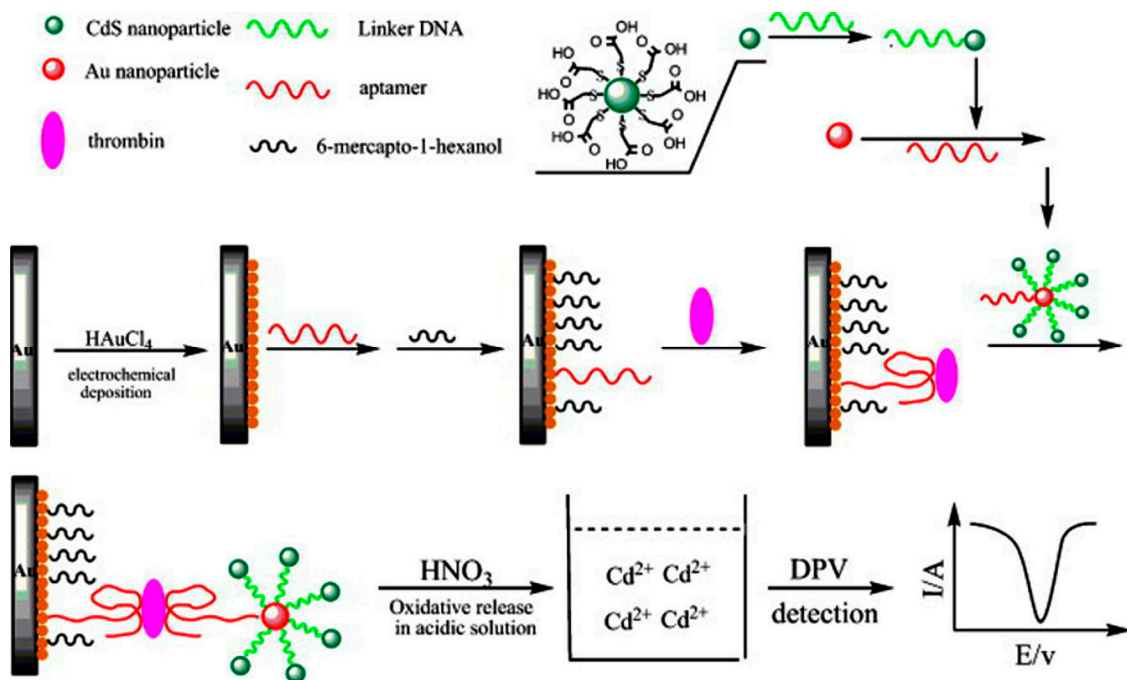


**Figure 1.** Scheme of an electrochemical method for the determination of thrombin based on aptamers forming a sandwich structure on an Au electrode covered by electrodeposited Au nanoparticles. The dissolution of CdS nanoparticles linked around gold nanoparticle labels releases  $\text{Cd}^{2+}$  ions that are detected by differential pulse voltammetry. Reprinted with permission from reference [46]. Copyright 2010 Elsevier.

In addition to alkaline phosphatase and horseradish peroxidase, other enzymes could be used to develop aptamer-based electrochemical assays. In one study, an enzyme for which the substrate is simply glucose was used to develop an assay [49]. An electrochemical sandwich assay for thrombin was based on pyroquinolinequinone glucose dehydrogenase, (PQQ)GDH. (PQQ)GDH was conjugated to biotinylated 29-mer aptamer using glutaraldehyde and used as the reporter. The 15-mer aptamer was used in a thiolated form and self-assembled onto a gold electrode surface. The enzyme-labeled detection aptamer was incubated together with thrombin in buffer and after washing the enzyme activity to added glucose was measured. Using 62 mM glucose in 10 mM 3-(N-morpholino)propanesulfonic acid (MOPS) buffer and chronoamperometric detection, a linear range from 40–100 nM was found with a detection limit of 10 nM.

Some electrochemical assays for thrombin have combined the use of an aptamer and an antibody. Both possibilities, aptamer as capture probe and antibody as capture probe have been reported. In one study [50], a nanostructured film of chitosan and gold nanoparticles was formed by electrodeposition from a solution of chitosan and  $\text{HAuCl}_4$  at  $-1$  to  $-3$  V (vs. SCE, saturated calomel electrode) for 2–6 min giving nanoparticles of diameter around 50 nm. A polyclonal sheep anti-thrombin antibody was then drop-cast onto the electrode, allowed to react, and then the remaining reactive sites blocked using BSA. The assay involved binding of thrombin to the antibody-modified electrode followed by binding of a 22-mer aptamer (170 nM) and then intercalation of methylene blue (MB) between the base pairs of the aptamer. The parameters for film formation and the concentrations of KCl and  $\text{MgCl}_2$  in the buffer solution were optimized, as the presence of  $\text{Mg}^{2+}$  promotes aptamer folding into stable G-quadruplexes that results in improved binding to thrombin. Using DPV to measure the peak current from the reduction of MB versus thrombin concentration gave a linear range from 1–60 nM and a detection limit of 0.5 nM. In contrast, an electrochemical sandwich assay combining an anti-thrombin antibody and 15-mer aptamer in which the aptamer served as the capture agent was reported [51]. The 15-mer aptamer had a long T tail of 20 base pairs terminated by



biotin on the 5'-end. Au nanoparticles of 13 nm diameter were prepared, and then anti-thrombin antibody and horseradish peroxidase were physisorbed onto the nanoparticles. Screen-printed electrodes (SPCE) were treated with  $\text{NH}_4\text{OH}$  to generate amine groups and then Au nanoparticles were adsorbed onto the surface and ferrocenedicarboxylic acid was added as a mediator. Streptavidin was then adsorbed onto the electrode surface followed by adsorption of the biotinylated aptamer. Thrombin samples were drop-cast onto the electrode and incubated at 4 °C for 1 h. The electrodes were then incubated with the enzyme and antibody-modified gold nanoparticles for 40 min. Detection of the bound nanoparticles was done using chronoamperometry to measure the current from the reduction of 3%  $\text{H}_2\text{O}_2$ . The detection of thrombin using this scheme was found to give a linear range from 10 pM to 100 nM with a detection limit of 1.5 pM. Thrombin spiked into human serum was able to be detected over a linear range from 100 pM–100 nM. An ultrasensitive and highly specific electrochemical aptamer-based assay for thrombin was designed based on the capture of  $\text{Fe}_3\text{O}_4/\text{Au}$  core-shell magnetic nanoparticles (AuMNPs) onto an Au electrode using a magnet [52]. AuMNPs were modified with the thiolated capture aptamers. The thiolated detection aptamer was immobilized on Au nanoparticles together with horseradish peroxidase (HRP). The formation of the sandwich structure including thrombin and the two aptamer labeled nanoparticles took place in solution and was followed by the capture of these sandwich complexes from 30  $\mu\text{L}$  of the solution drop-cast onto the Au working electrode and collected onto the electrode surface using a magnet. After the addition of 1 mL of solution containing hydroquinone and  $\text{H}_2\text{O}_2$ , detection of benzoquinone by DPV was done after a 5 min incubation. The assay was able to detect thrombin over a linear range of 0.1–60 pM and with a detection limit of 30 fM as shown in Figure 2.

The use of a sandwich between the primary aptamer and antibody-modified magnetic nanoferrite nanoparticles was introduced as a means of achieving much faster analysis times [53]. Screen-printed electrodes (SPCE) were modified with a conducting polymer (poly-(2,2':5',5''-terthiophene-3'-p-benzoic acid)) and the amine-terminated aptamer conjugated to the polymer using EDC/NHS chemistry. The nanoferrite particles were modified by starch with attached streptavidin proteins for binding of biotinylated antibodies. The hydroxyl groups of the nanoparticles were activated by carbonyl-diimidazole for binding to toluidine blue O (TBO) which would serve as a redox marker. The analysis parameters were optimized and found to be 3 min for thrombin binding followed by 4 min of binding of the magnetic nanoparticles with the magnetic field followed by 10 s of reversed magnetic field to remove magnetic nanoparticles not bound by antibody–thrombin interaction. The current due to reduction of TBO was used as the signal and a linear range of 1–500 nM was found with a detection limit of 0.49 nM.

An approach to signal amplification in an aptamer sandwich assay for thrombin was based on having the reporter aptamer bound to gold nanoparticles decorating the surface of microparticles of hollow  $\text{CeO}_2$  capable of catalyzing the reduction of  $\text{H}_2\text{O}_2$  [54]. Indium tin oxide (ITO) electrodes were dip-coated with Ag nanowires ( $d = 80 \text{ nm}$ ,  $l = 20 \mu\text{m}$ ) for three cycles and then modified with the amine-terminated capture aptamer. The highly conductive Ag nanowires helped to enhance the electrochemical signal. The hollow  $\text{CeO}_2$  microparticles ( $d \sim 1 \mu\text{m}$ ) were prepared by template synthesis and then served as templates for decoration with Au nanoparticles onto which the thiolated reporter aptamer was bound. The detection was achieved using DPV in 10 mM  $\text{H}_2\text{O}_2$  after a 40 min thrombin binding time. The arrangement of the components for this assay is depicted in Figure 3. A linear relation was found between the current due to  $\text{H}_2\text{O}_2$  reduction and  $\log$  [thrombin] over the range 0.5 pM–30 nM with a detection limit of 0.25 pM.

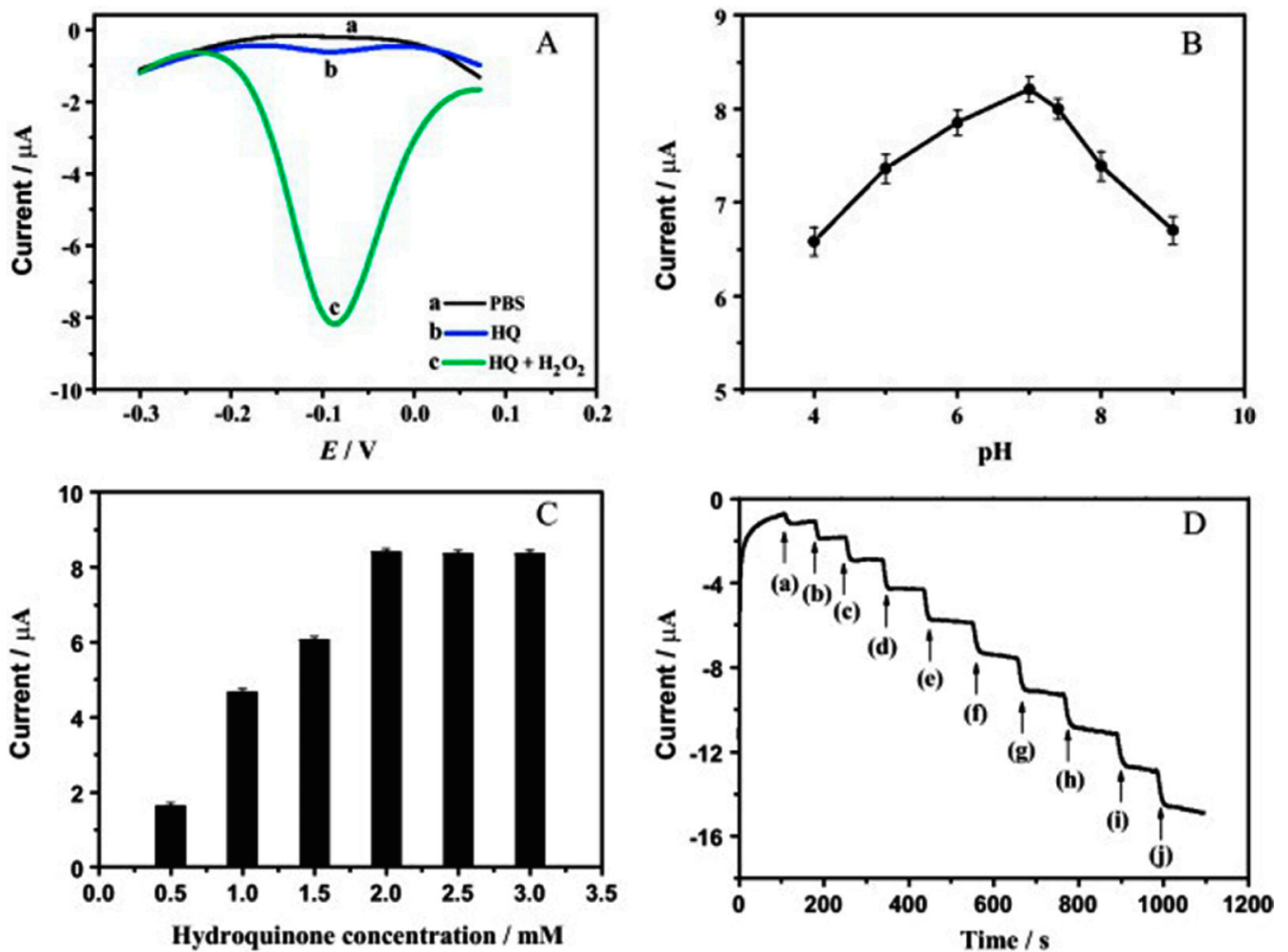


**Figure 2.** (A) Differential pulse voltammograms of an AuMNPs-Apt1/thrombin/Apt2-AuNPs-HRP-modified gold electrode in solution of pH 7.0 PBS containing (a) no  $\text{H}_2\text{O}_2$  and hydroquinone (HQ), (b) 2 mM HQ, and (c) 1.5 mM  $\text{H}_2\text{O}_2$  + 2 mM HQ. (B) The current response of the aptasensor in PBS containing 2 mM HQ and 1.5 mM  $\text{H}_2\text{O}_2$  at different pH values. (C) The current response of the aptasensor in PBS (pH 7.0) containing different HQ concentrations. (D) The current response of the aptasensors in PBS (pH 7.0) at the potential of  $-0.2$  V while  $\text{H}_2\text{O}_2$  was stepwise added into the system. The final concentration of  $\text{H}_2\text{O}_2$  reaches to (a) 0.25, (b) 0.5, (c) 0.75, (d) 1.0, (e) 1.25, (f) 1.5, (g) 1.75, (h) 2.0, (i) 2.25, and (j) 2.5 mM. Reprinted with permission from reference [52]. Copyright Elsevier 2011.

A summary of the results obtained for the detection of thrombin using aptamers and electrochemical sandwich assay approaches is presented in Table 1. In certain studies, both a very low detection limit and a wide linear range have been reported, conditions needed for a successful assay.

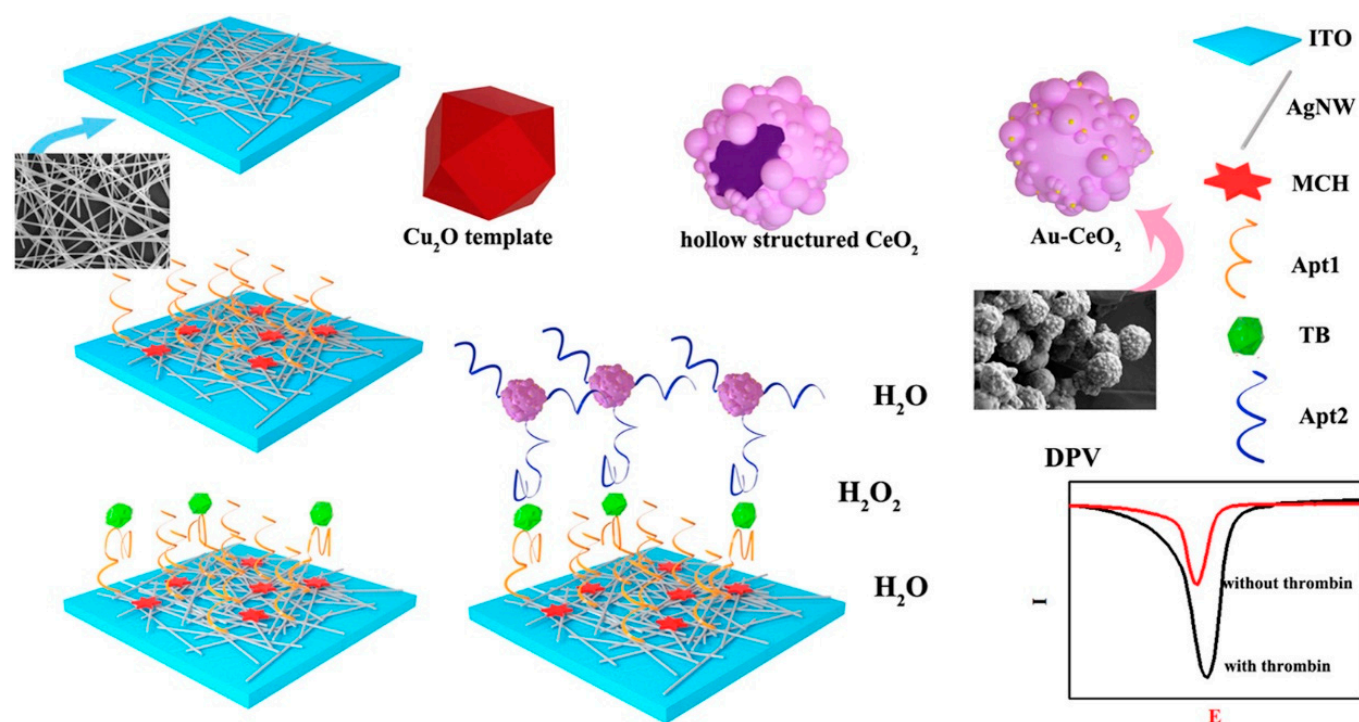


**Figure 3.** Schematic of an electrochemical assay for thrombin (TB) based on indium tin oxide electrodes (ITO) first modified with Ag nanowires (AgNW) onto which the capture aptamer is bound along with mercaptohexanol (MCH). The Cu<sub>2</sub>O particle is a template for formation of hollow CeO<sub>2</sub> particles that are decorated with Au nanoparticles. Detection of catalysis of reduction of H<sub>2</sub>O<sub>2</sub> by CeO<sub>2</sub> is done using differential pulse voltammetry. Reprinted with the permission from reference [54]. Copyright Elsevier 2020.

**Table 1.** Electrochemical Sandwich Assays for Thrombin using Aptamers.

Components of Sandwich Assay for Thrombin (Th = Thrombin, SAM = Self-Assembled Monolayer)	Method of Detection	Linear Range	Limit of Detection	Ref.
Au/SAM/Aptamer covalently attached to methylene blue (not a sandwich assay, for comparison only)	AC voltammetry	6.4 nM–768 nM	6.4 nM	[35]
Au/thiolated aptamer/Th/aptamer-modified gold nanoparticles with adsorbed rhodamine 6G	Electrochemical Impedance Spectroscopy	0.05–18 nM	0.02 nM	[38]
Au/thiolated aptamer/Th/glucose dehydrogenase (GDH)-labeled aptamer (glucose substrate)	Amperometry	nonlinear	1 μM	[39]
Au/mixed SAM with thiolated aptamer/Th/aptamer labeled CdS quantum dots	Potentiometry	100 pM–1 nM	0.14 nM	[40]
Au electrode/thiolated aptamer/Th/graphene modified Au nanoparticles with reporter aptamer	Electrochemical Impedance Spectroscopy	0.3–50 nM	0.01 nM	[41]
Nanoporous Au/thiolated aptamer in mixed SAM/Th/aptamer-modified Au nanoparticles	Chronocoulometry	0.01–22 nM	30 fM	[42]
Screen-printed carbon electrode/streptavidin coated magnetic beads/5'-biotinylated primary aptamer/Th/5'-biotinylated secondary aptamer/streptavidin-alkaline phosphatase conjugate	Differential pulse voltammetry	0.1–100 nM (non-linear)	0.45 nM	[44]
Screen-printed carbon electrode, streptavidin-coated magnetic beads, thrombin, biotinylated thrombin, streptavidin-alkaline phosphatase conjugate, β-Ala-Gly-Arg-p-nitroaniline (thrombin substrate) (not sandwich, indirect and direct competitive assay for comparison)	Differential pulse voltammetry	0–2000 nM (not linear) N/A 100–600 nM studied	430 nM (direct) not successful (indirect) 175 nM (thrombin product detection)	[45]
Au/thiolated aptamer in mixed SAM/Th/Au nanoparticles modified with aptamer and DNA linked CdS nanoparticles	Differential pulse voltammetry	1.0 fM–10 pM	0.55 fM	[46]

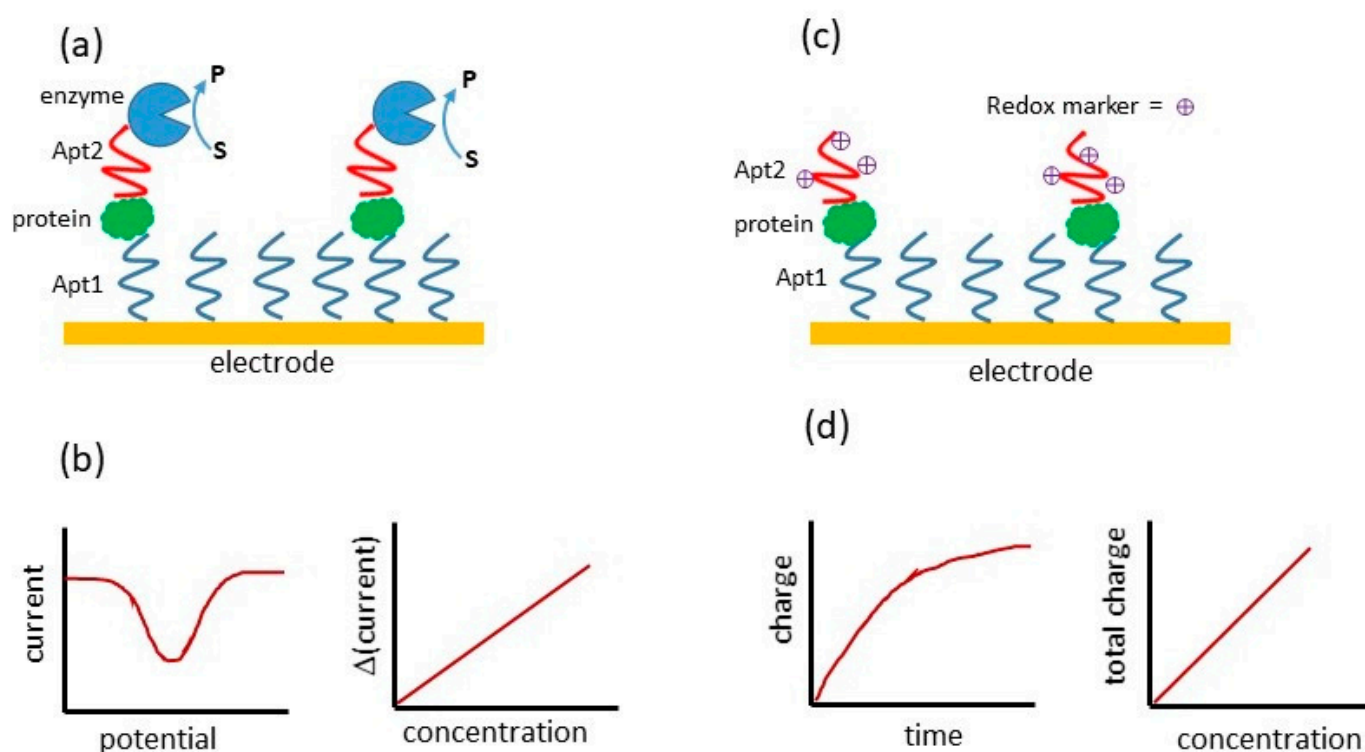
Table 1. Cont.

Components of Sandwich Assay for Thrombin (Th = Thrombin, SAM = Self-Assembled Monolayer)	Method of Detection	Linear Range	Limit of Detection	Ref.
Au/thiolated aptamer/Th/Pt nanoparticle decorated carbon nanocages	Differential pulse voltammetry	0.05 pM–20 nM	10 fM	[47]
Glassy carbon electrode/graphene oxide sheets doped with nitrogen and sulfur decorated with gold nanoparticles/thiolated aptamer/Th/graphene oxide sheets doped with nitrogen and sulfur decorated with gold nanoparticles modified by thiolated secondary aptamer and thiolated biotinylated DNA/avidin-horseradish peroxidase conjugate	Differential pulse voltammetry	0.1 pM–10 nM (vs. log[Th])	25 fM	[48]
Au/thiolated aptamer/Th/pyrroquinoline quinone glucose dehydrogenase labeled secondary aptamer	Chrono-amperometry	40–100 nM	10 nM	[49]
Glassy carbon electrode/chitosan-nanogold film/cross-linked antibody/Th/secondary aptamer and methylene blue	Differential pulse voltammetry	1–60 nM	0.5 nM	[50]
Screen-printed carbon electrode/Au nanoparticles and ferrocene dicarboxylic acid mediator/streptavidin/biotinylated aptamer/Th/Au nanoparticles modified with horseradish peroxidase-antibody conjugates	Chrono-amperometry	10 pM–0.1 $\mu$ M	1.5 pM	[51]
Au/core-shell Fe <sub>3</sub> O <sub>4</sub> /Au magnetic nanoparticles modified with primary aptamer/Th/Au nanoparticles labeled with secondary aptamer and horseradish peroxidase	Differential pulse voltammetry	0.1–60 pM	30 fM	[52]
Screen-printed carbon electrodes/conducting polymer layer conjugated to primary aptamer/Th/streptavidin–starch coated magnetic nanoparticles and biotinylated secondary aptamer, toluidine blue O	Chrono-amperometry	1.0–500 nM	0.49 nM	[53]
Indium tin oxide electrodes/Ag nanowires/amino-functionalized primary aptamer/Th/Au nanoparticles on hollow CeO <sub>2</sub> structures with secondary aptamer	Differential pulse voltammetry	0.5 pM–30 nM	0.25 pM	[54]

### 3. Other Electrochemical Sandwich Assays Using Two Aptamers

Strategies using two aptamers have been applied to develop assays for a number of other analytes ranging from small molecules to biomolecules to cells but with a particular focus on protein biomarkers. The surfaces on which the primary (capture) aptamer is immobilized have included self-assembled monolayers on Au electrode surfaces, electrodeposited Au nanoparticles, and on a variety of nanostructured surfaces and nanocomposite materials of high surface area or improved conductivity supported on electrodes such as glassy carbon. The secondary aptamer (detection, or reporter aptamer) has been applied in many forms, including conjugated to enzymes through the biotin–streptavidin interaction and also bound around nanoparticles to provide amplification or for the nanoparticles themselves to be used as electrochemical tags. The aptamers themselves are often modified, being thiolated, biotinylated, or bearing a redox-active tag. In the simplest approach for a sandwich assay using two aptamers, the most common electrochemical measurement technique used is differential pulse voltammetry to detect an enzyme product produced by an enzyme associated with the detection aptamer in the presence of added substrate. Another approach uses chronocoulometry to detect charge associated with the binding of a redox marker by electrostatic interactions. These two basic assay architectures are shown in Scheme 2. In more elaborate architectures in which a double-stranded DNA is formed in a hybridization step, a redox marker that intercalates into the dsDNA can be used.





**Scheme 2.** The basic architectures for electrochemical sandwich assays consisting of a capture aptamer (Apt1) and a detection aptamer (Apt2). In the scheme shown in (a), the detection aptamer is bound to an enzyme and the enzyme product is detected using differential pulse voltammetry, with the difference in current in the presence and absence of protein plotted versus analyte concentration over the linear range, as shown in (b). In the scheme shown in (c), a redox marker binds electrostatically to the detection aptamer and is detected using chronocoulometry which measures charge vs. time in the initial measurement with total charge passed plotted vs. analyte concentration over the linear range, as shown in (d).

A two aptamer sandwich assay was developed for a form of platelet-derived growth factor (PDGF), useful as a biomarker for cancer and renal function deterioration [55]. The surface of a glassy carbon electrode (GCE) was drop-cast with a 0.1% chitosan solution containing carbon aerogel (CA) mesoporous carbon material incorporating MoS<sub>2</sub> nanoflowers that provided excellent conductivity and increased the surface area. The chitosan was used to immobilize gold nanoparticles modified with the thiolated capture aptamer. The reporter and capture aptamer were the same 45-mer with hexanethiol at the 5'-end. The PDGF protein form detected was a dimer with two identical disulfide-linked subunits and hence using the same aptamer for capture and reporting was suitable. The reporter aptamers were attached to gold nanoparticles together with 6-ferrocenyl hexanethiol. The assay was performed using a 2-h incubation time in the PDGF solution with the capture aptamer-modified electrode followed by an additional 2 h incubation with the reported aptamer-modified gold nanoparticles, providing the results shown in Figure 4. Cyclic voltammetry or DPV was done in the presence of dissolved [Fe(CN)<sub>6</sub>]<sup>3-/4-</sup> serving as a mediator. A detection limit of 0.3 pM was achieved along with a linear range from 0.001–10 nM. The determination of PDGF using the biosensor in three human serum samples diluted into PBS from healthy donors and two from patients was found to agree well, better than 5%, with the amount determined by a standard ELISA assay.

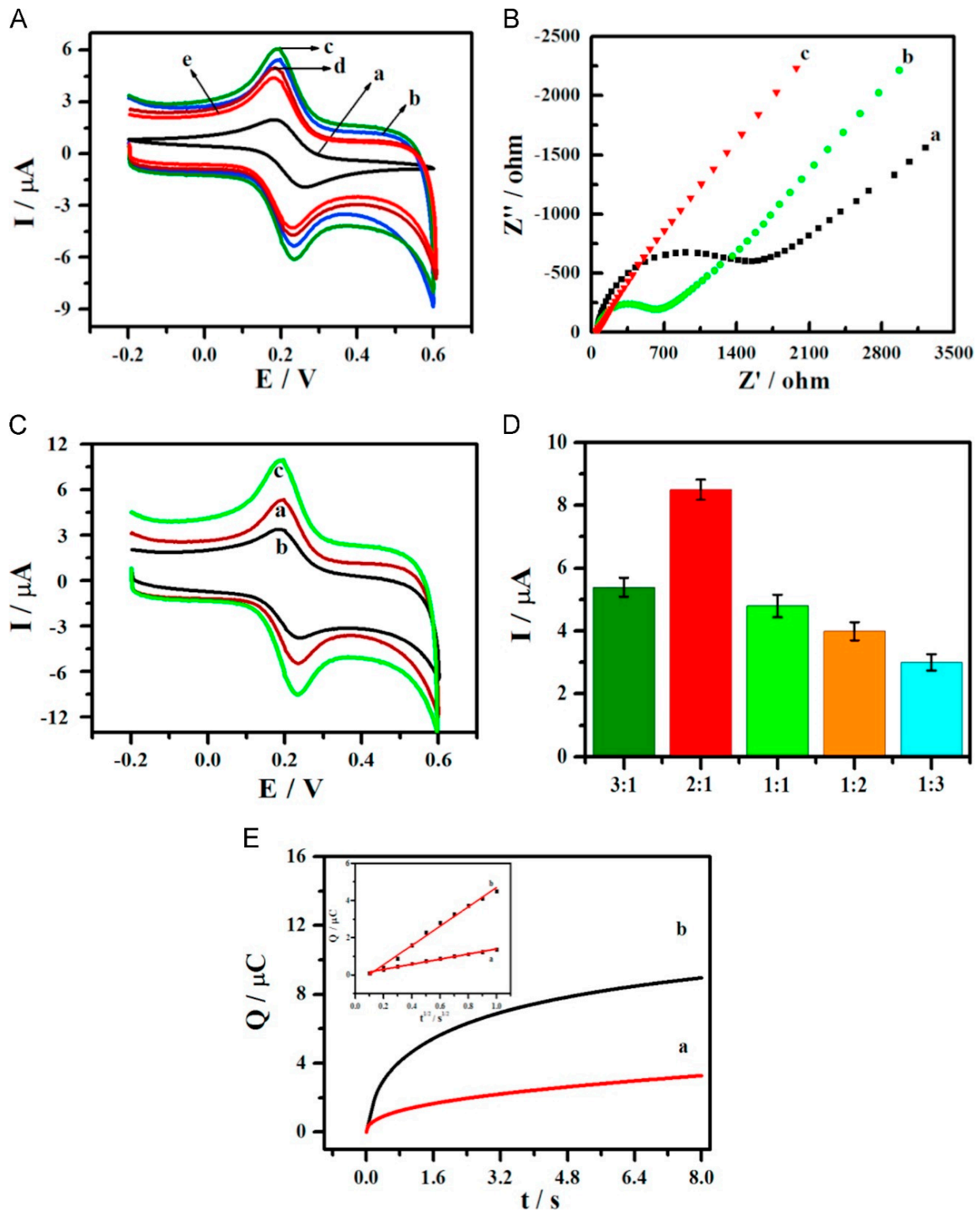


**Figure 4.** (A) CV of different electrodes at a scan rate of  $50 \text{ mV s}^{-1}$ : (a) GCE, (b)  $\text{MoS}_2/\text{CA}/\text{GCE}$ , (c)  $\text{AuNPs}/\text{MoS}_2/\text{CA}/\text{GCE}$ , (d)  $\text{Apt1}/\text{AuNPs}/\text{MoS}_2/\text{CA}/\text{GCE}$ , (e)  $\text{BSA}/\text{Apt1}/\text{AuNPs}/\text{MoS}_2/\text{CA}/\text{GCE}$ ; (B) Nyquist plots of bare GCE (a),  $\text{MoS}_2/\text{CA}/\text{GCE}$  (b),  $\text{AuNPs}/\text{MoS}_2/\text{CA}/\text{GCE}$ ; (C) CV of  $\text{BSA}/\text{Apt1}/\text{AuNPs}/\text{MoS}_2/\text{CA}/\text{GCE}$  (a),  $\text{PGDF-BB}/\text{BSA}/\text{Apt1}/\text{AuNPs}/\text{MoS}_2/\text{CA}/\text{GCE}$  (b),  $\text{Fc-AuNPs-Apt2}/\text{PGDF}/\text{BB}/\text{BSA}/\text{Apt1}/\text{AuNPs}/\text{MoS}_2/\text{CA}/\text{GCE}$ ; (D) DPV response to the different volume proportions of AuNP-modified Fc (5 mM) and Apt 2 (1  $\mu\text{M}$ ); (E) Plot of  $Q-t$  curves of the (a) GCE and (b)  $\text{AuNPs}/\text{MoS}_2/\text{CA}/\text{GCE}$ . Inset plot of  $Q-t^{1/2}$  curves on (a) GCE and (b)  $\text{AuNPs}/\text{MoS}_2/\text{CA}/\text{GCE}$ . Reprinted with permission from reference [55]. Copyright Elsevier 2015.

Neutrophil gelatinase-associated lipocalin (NGAL or lipocalin-2) protein is a potential biomarker for pancreatic adenocarcinoma (PADC), and hepatocellular carcinoma in combination with other biomarkers. Two different NGAL aptamers were used in direct sandwich and competitive assay formats on Au electrodes and magnetic beads. A sandwich assay using capture aptamer on magnetic beads and a reporter aptamer tagged with biotin or with 6-carboxyfluorescein that would bind to either a peroxidase–streptavidin conjugate or to a peroxidase–anti-FC-peroxidase conjugate was found to show large currents in the absence of NGAL, attributed to possible aptamer hybridization. Using truncated aptamers, similar currents were seen in the presence or absence of NGAL [56]. Detection of lipocalin-2, also known as a biomarker for renal failure, was achieved using an electrochemical aptamer sandwich assay [57]. A graphite screen-printed electrode was modified by a layer of conducting polymer formed by electropolymerization onto which a layer of gold nanoparticles was formed by electrodeposition. The gold nanoparticles were modified by a first aptamer that would bind lipocalin-2. After the binding of lipocalin-2, a second aptamer conjugated to biotin was bound to form a sandwich. Streptavidin conjugated to alkaline phosphatase was applied and using 1-naphthylphosphate as an enzyme substrate yielded 1-naphthol that could then be detected by oxidation in DPV yielding a linear range from 1.0–1000 ng mL<sup>-1</sup> and a detection limit of 0.3 ng mL<sup>-1</sup>.

An electrochemical aptasensor for immunoglobulin E (IgE) was fabricated using enzyme-linked aptamer in a sandwich assay format [58]. First, an amide-terminated capture aptamer and thionine (redox mediator) were covalently attached to the amine functional group of chitosan via amide bond formation using phthaloyl chloride as linker on glassy carbon electrode (GCE) modified with multi-walled carbon nanotubes (MWCNT)/ionic liquid (IL)/chitosan nanocomposite. The biotin–streptavidin interaction was used to attach another IgE aptamer with biotin and horseradish peroxidase (HRP). HRP has been used as a label for signal amplification and catalyzing the oxidation of thionine by hydrogen peroxide. The presence of IgE induces the formation of a sandwich structure on the electrode and was monitored by electrochemical impedance spectroscopy (EIS) and cyclic voltammetry (CV) and differential pulse voltammetry as shown in Figure 5. The limit of detection found was 6 pM with a sensitivity of 1.88  $\mu\text{A nM}^{-1}$  at a range up to 20 nM. The proposed aptasensor was used to detect IgE in human serum as other proteins such as lysosome and bovine serum albumin (BSA) did not interfere with the detection of IgE.

An electrochemical aptamer-based assay for the detection of both total and glycated hemoglobin in blood has been reported [59]. A blood concentration of the glycated form of hemoglobin (HbA1c) of over 6.5% is one of the criteria for the diagnosis of diabetes. A higher amount of HbA1c is associated with other diseases including cardiovascular disease, nephropathy, and retinopathy. Thiol-modified forms of the aptamers were immobilized on gold nanoparticle-modified array electrodes. A new DNA aptamer against HbA1c and tHb was identified and characterized from a 60-mer library with dissociation constants of 2.8 nM and 2.7 nM for HbA1c and tHb, respectively. The aptasensor voltammetry response towards tHb and HbA1c was measured in the concentration range of 100 pg mL<sup>-1</sup>–10  $\mu\text{g mL}^{-1}$ . Detection limits for tHb of 0.34 ng mL<sup>-1</sup> and 0.2 ng mL<sup>-1</sup> for HbA1c were found. The detection of the HbA1c in whole blood samples was also carried out showing its potential application to discriminate between diabetic and healthy individuals.

Recently, an electrochemical assay capable of detecting the glycosylation of prostate-specific antigen (PSA) using two aptamers in a sandwich format was developed [60]. Biotinylated aptamer was immobilized on a gold electrode by conjugation to a self-assembled monolayer followed by incubation with serial dilutions of a standard PSA solution followed by binding of the detection aptamer, which was labeled with 6-carboxyfluorescein that would bind to a Fab anti-fluorescein–peroxidase conjugate. The enzyme substrate used to generate the detection current was 3, 3', 5, 5'-tetramethylbenzidine (TMB). A novel DNA aptamer was isolated targeting human PSA (hPSA) by a counter-selection process using recombinant PSA (rPSA) that does not carry the glycan moiety, thus selecting for an aptamer that bound both to regions of the protein and the glycan. The selected aptamer

was tested using an electrochemical binding assay with chronoamperometric detection. The range of detection for hPSA was 0.66–62.5 ng mL<sup>-1</sup> in TBS buffer and 0.66–25 ng mL<sup>-1</sup> in diluted serum with a detection limit of 0.66 ng mL<sup>-1</sup>. The response of the assay to rPSA was very low as the glycan was absent. The sensor supported measurement in serum samples with minimum dilution which allows evaluation of the PSA levels in the diagnosis of prostate cancer. A subsequent study presented a computational prediction of the structure of the aptamer and of its complex with the glycoprotein [61].

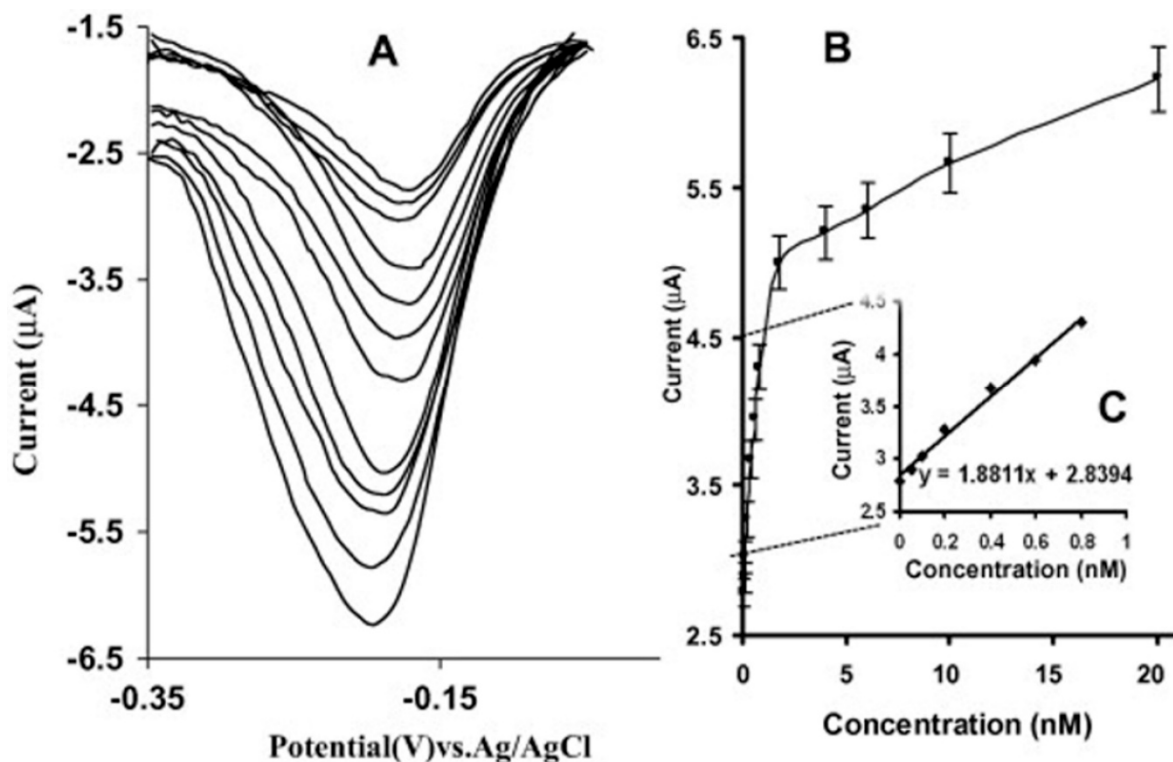


**Figure 5.** (A) Differential pulse voltammograms of SA-HRP-biotin aptamer/IgE/NH<sub>2</sub> aptamer/MWCNT/IL/Chit/GC electrode after incubation for 15 min with different IgG concentrations (from inner to outer: 0, 0.05, 0.1, 0.2, 0.4, 0.6, 0.8, 2, 4, 6, 10, and 20 nM) in PBS (0.1 M, pH 7.4) containing 2.5 mM H<sub>2</sub>O<sub>2</sub>. (B) Plot of current response vs. IgE concentration. (C) The linear portion of the current versus IgE concentration response. Reprinted with permission from reference [58]. Copyright, 2014 Elsevier.

The detection of adenosine triphosphate was performed on a nanoporous gold electrode using 3,4-diaminobenzoic acid (DABA) as a molecular reporter in the aptamer-based electrochemical biosensor [62]. The ATP binding aptamer was split into two fragments and the first fragment was immobilized on the nanoporous gold surface and the second fragment was covalently bound to the activated carboxylic end of DABA using EDC/NHS chemistry. A 27-mer ATP binding aptamer was split into two fragments and these two fragments fold around the ATP. The electrochemical signal was generated by the oxidation of DABA and due to a nine-fold higher surface area of the nanoporous gold electrode compared to the geometric area of the electrode, the signal was amplified due to the loading of more DABA molecules. The nanoporous gold electrode was prepared by anodization by applying a step potential from open circuit potential to 4V followed by the reduction of gold oxide to metallic gold using ascorbic acid. The limit of detection of the sensor was 100 nM without significant interference from the other similar nucleotide analogs.

Cardiac troponin (cTnI) is a protein found in heart muscle and when released into the blood it serves as a biomarker for myocardial infarction and can remain in the myocardial tissue for 10 days. An electrochemical dual-aptamer-based biosensor was proposed for the analysis of cTnI based on using DNA nanotetrahedron (NTH) capture probes and



multifunctional hybrid probes [63]. NTHs presenting the Tro4 aptamer were immobilized on a screen-printed gold electrode (SPGE). Magnetic Fe<sub>3</sub>O<sub>4</sub> nanoparticles were used as nanocarriers to load the larger amount of cTnI-specific Tro6 aptamer, HRP, HRP-mimicking Au@Pt nanoenzyme and G-quadruplex/hemin DNAzyme as the hybrid nanoprobe. The target cTnI was sandwiched between the two types of aptamers (Tro4 and Tro6) and the electrochemical signal from DPV was measured by immersing in the detection solution containing hydroquinone (HQ), which was oxidized to benzoquinone (BQ) with H<sub>2</sub>O<sub>2</sub> in the enzymatic reactions of the numerous HRP, HRP-like nanoenzymes and DNAzymes. Tro4 aptamer probes are built onto one of the NTH sequences, and the other 3 DNAs present thiol groups for bonding to the Au surface. The use of NTH results in well-spaced aptamer presentation on the electrode surface. The dynamic range of detection was 0.01–100 ng mL<sup>-1</sup> and the limit of detection was 7.5 pg mL<sup>-1</sup>. In a related study, cTnI was analyzed using an aptasensor based on DNA NTH linked dual-aptamer and magnetic metal–organic frameworks of type Fe<sub>3</sub>O<sub>4</sub>@UiO-66 decorated by Au@Pt nanoparticles, HRP, G-quadruplex/hemin DNAzyme and Tro4 and Tro6 aptamers. The dynamic range of detection was 0.01–100 ng mL<sup>-1</sup> and the limit of detection was 5.7 pg mL<sup>-1</sup> [64]. The assembly of the components for this assay is shown in Figure 6. An electrochemical biosensor for cTnI was also created on SPCE coated with a carboxyethylsilanetriol-modified graphene oxide and detection was achieved using an aptamer-biomarker-enzyme labeled aptamer sandwich scheme [65]. An amine-terminated capture aptamer was covalently attached to the modified graphene oxide sheets using EDC/NHS chemistry. Ethanolamine was used as a capping agent and casein was used as a blocking agent. The detection aptamer was conjugated to horseradish peroxidase. The amperometric current was recorded at –200 mV (vs. Ag/AgCl) in the presence of H<sub>2</sub>O<sub>2</sub> and hydroquinone in pH 7.6 buffer. For measurement in human serum spiked with cTnI, a detection limit of 3.4 pg mL<sup>-1</sup> was reported with a linear range extending up to 1.0 µg mL<sup>-1</sup>. The selectivity against four other common blood proteins (C-reactive protein, human serum albumin, myoglobin, immunoglobulin G) was tested and the signal associated with each of these four proteins was found to be less than 20% of the signal due to cTnI. Another electrochemical biosensor for cTnI was designed based on the reduction of H<sub>2</sub>O<sub>2</sub> by hydrazine [66]. SPCE were modified with 5 nm Au nanoparticles by drop-casting followed by potential cycling to achieve electrostatic deposition. A layer of conducting polymer was then formed by potential cycling in the presence of the 5,2':5',2''-terthiophene-3'-carboxylic acid monomer. The Tro4 aptamer was conjugated to the polymer layer through the 5'-amine end using EDC/NHS chemistry and served as the capture aptamer. The Tro6 aptamer was 5'-phosphate modified and then linked to adipic acid dihydrazide through a phosphoramidate bond. The reaction between the hydrazine labeled Tro6 detection aptamer and H<sub>2</sub>O<sub>2</sub> was detected using chronoamperometry. A detection limit of 1.0 pM was achieved and a linear range of 1–100 pM. The limit of detection was below that of commercial immunoassay kits for cTnI.

A highly sensitive electrochemical sandwich assay for human epidermal growth factor 2 (HER2), a biomarker for breast cancer, was developed using two aptamers and a combination of nanoflowers functioning as nanozymes [67]. Thiolated DNA nanotetrahedrons were assembled onto a gold electrode presenting the capture aptamer. Nanoflowers of Mn<sub>3</sub>O<sub>4</sub> coated by a layer of poly(diallyldimethylammonium chloride) were prepared of size 100 nm and decorated with 40 nm Pd@Pt nanoflowers functioning as nanozymes followed by assembly of the detection aptamer and horseradish peroxidase onto these particles. The three-component nanocatalyst was designed to very effectively catalyze the reaction of hydroquinone with H<sub>2</sub>O<sub>2</sub> to form benzoquinone. Following the formation of the sandwich structure and additional complementary DNA strand terminated in Pd@Pt nanoflower was hybridized to the detection aptamer to further enhance the signal. A detection limit of 0.08 ng mL<sup>-1</sup>, the lowest yet reported for HER2, and a linear range of 0.1–100 ng mL<sup>-1</sup> was reported. Agreement with ELISA kits was within 5–8% for HER2 spiked into diluted human serum samples. The relevant diagnostic range for HER2 was noted as 4–75 ng mL<sup>-1</sup>.

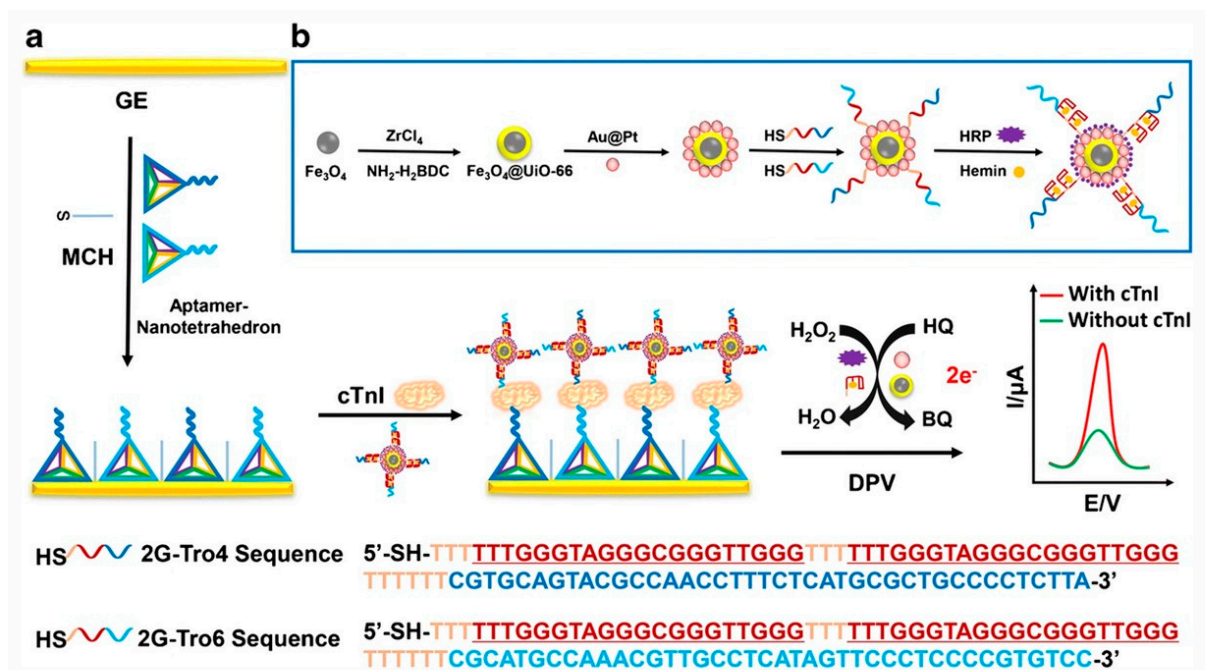


**Figure 6.** Schematic of the electrochemical sandwich assay for cardiac troponin I (cTnI) in which the capture aptamer is a thiolated DNA nanotetrahedron with one aptamer strand. The detection aptamer is bound to Au@Pt nanoparticles around magnetic metal organic framework ( $\text{Fe}_3\text{O}_4@UiO-66$ ) particles bound to Tro4 and Tro6 aptamers along with G-quadruplex/hemin (GQH) DNAzyme and horseradish peroxidase (HRP). Pathway (a) shows the steps for the modification of the screen-printed gold electrodes with DNA nanotetrahedrons presenting the Tro4 aptamer, the formation of the sandwich structure with cTnI and the modified  $\text{Fe}_3\text{O}_4$  nanoparticles presenting the Tro6 aptamer and enzymes. The sequences for Tro4 and Tro6 are shown at the bottom of the figure. Pathway (b) shows the steps for the production of the Tro6 modified aptamer-labeled nanoparticles and enzymes for detection. Reproduced with permission from [64]. Copyright Springer 2019.

An aptamer sandwich assay for cocaine was developed that included enzymatic redox-cycling for signal amplification [68]. SPCE were drop coated with graphene oxide that was then reduced to graphene followed by electrodeposition of gold nanoparticles from a solution of  $\text{HAuCl}_4$  precursor. A thiolated cocaine binding aptamer was then self-assembled onto the gold nanoparticles. The electrodes were incubated for 40 min with concentrations of cocaine and a second cocaine binding aptamer that was biotinylated. Alkaline phosphatase (ALP) conjugated to streptavidin was then bound to the sandwich complex and the enzyme substrate p-aminophenyl phosphate (p-APP) and NADH were introduced. ALP catalyzed the conversion of p-APP to p-aminophenol that was then oxidized on the electrode surface to p-quinoneimine. The presence of NADH caused conversion of p-quinoneimine to p-aminophenol resulting in enhanced current response during a DPV sweep. A linear range from 1–500 nM was found with a detection limit of 1 nM.

An aptamer sandwich approach was used to detect MCF-7 human breast cancer cells [69]. A thiolated MUC1 (mucin glycoprotein) aptamer was assembled on gold electrodes. The cell suspension was incubated with the electrode for 2 h and after non-specifically bound cells were washed away incubation with MUC1 aptamer conjugated to horseradish peroxidase was done. In the presence of thionine as an electron transfer mediator, the catalytic current observed by cyclic voltammetry arising from the reduction of  $\text{H}_2\text{O}_2$  was linear with respect to  $\log(\text{cell count})$  with a detection limit of 100 cells and a range from  $100-10^7$  cells. Another dual aptamer-based sandwich biosensor was constructed to detect MCF-7 breast cancer cells using the MUC1 tumor marker [70]. MUC1 binding aptamer was immobilized on the surface of GCE modified with a multi-walled carbon nanotube/poly(glutamic acid) composite. Cancer cells were sandwiched between

capture aptamer and AgNPs linked to detection aptamer by glutathione. The captured Ag nanoparticles were dissolved by 0.5 M HNO<sub>3</sub> and then detection of Ag<sup>+</sup> was carried out using differential pulse voltammetry. The concentration range of the detection was 1.0 × 10<sup>2</sup> to 1.0 × 10<sup>7</sup> cells mL<sup>-1</sup> with a detection limit of 25 cells.

The detection of *S. aureus* using a primary and secondary aptamer sandwich assay was reported [71]. The primary aptamer was immobilized on magnetic beads and the secondary aptamer was bound to silver nanoparticles. The capture bacteria and attached silver nanoparticles were treated in acid to dissolve the silver nanoparticles followed by detection of the Ag<sup>+</sup> ion by stripping voltammetry. A detection range from 10–1 × 10<sup>6</sup> CFU mL<sup>-1</sup> was obtained with a detection limit of 10 CFU mL<sup>-1</sup>. Results for real water samples containing *S. aureus* were found to be consistent with those found using the assay.

The detection of type 2 diabetes biomarker vaspin using an electrode modified by a high surface area natural biomineral structure (coccolith) from *Emiliania huxleyi*, an ocean unicell organism [72]. The coccoliths were drop-cast on a screen-printed gold electrode and then sputter-coated with gold. A pair of aptamers binding to different epitopes on vaspin was used in the sandwich assay, with the first aptamer drop-cast and then after vaspin binding, the second aptamer conjugated to enzyme HRP was added. The electrochemical signal was the oxidation of substrate TMB in the presence of H<sub>2</sub>O<sub>2</sub> achieving a detection limit of 298 pM.

An electrochemical sandwich assay for lysozyme was developed using two aptamers [73]. Abnormal concentrations of lysozyme can serve as a biomarker for a range of diseases. A thiol terminated lysozyme binding aptamer (LBA, of sequence: 5'-SH-(CH<sub>2</sub>)<sub>6</sub>-ATC-TAC-GAA-TTC-ATC-AGG-GCT-AAA-GAG-TGC-AGA-GTT-ACT-TAG-3') and horseradish peroxidase was loaded onto Au nanoparticles of average size 18 nm. LBA and dithiothreitol were drop-cast onto a flat gold electrode and then surface blocking was carried out using mercaptohexanol. EIS was used to confirm the binding of lysozyme to the aptamer-modified electrode and then the binding of the Au-LBA-HRP conjugates. The parameters of hydroquinone concentration, H<sub>2</sub>O<sub>2</sub> concentration, pH, immersion time and amount of HRP were all optimized to produce the largest DPV signal. Detection was performed using DPV in 150 mM H<sub>2</sub>O<sub>2</sub> and 30 mM hydroquinone. A linear dependence of the increase in DPV peak current with log[lysozyme] was found from 0.01 pg mL<sup>-1</sup> to 105 pg mL<sup>-1</sup> with a detection limit of 0.003 pg mL<sup>-1</sup>. The selectivity of the aptasensor against interfering species (thrombin, BSA, glucose, cytochrome *c*, immunoglobulin G, ATP) was found to be good and recovery of lysozyme from human serum samples in the range 85%–108% was reported.

A summary of the results for these studies of biological analyte detection using aptamers in a sandwich configuration and electrochemical methods is presented in Table 2.

**Table 2.** Electrochemical Sandwich Assays Using Two Aptamers.

Analyte	Components of Sandwich Assay	Method of Detection	Linear Range	Limit of Detection	Ref.
Platelet-Derived Growth Factor BB (PDGF-BB)	Glassy carbon electrode/carbon aerogel-MoS <sub>2</sub> composite with Au nanoparticles/primary aptamer/PDGF-BB/Au nanoparticles with secondary aptamer and 6-ferrocenylhexanethiol	Cyclic voltammetry	0.001–10 nM	0.3 pM	[55]
Lipocalin-2	Screen-printed Au electrode/magnetic beads coated with capture aptamer/lipocalin-2/reporter aptamer tagged with biotin or 6-carboxyfluorescein /peroxidase label (either by streptavidin conjugate or Fab-antiFITC conjugate)	Chrono-amperometry	N/A	N/A	[56]
Lipocalin-2	Graphite screen-printed electrode/conducting polymer/Au nanoparticles/thiolated aptamer/lipocalin-2/biotinylated aptamer/alkaline phosphatase-streptavidin conjugate	Differential pulse voltammetry	1–1000 ng/mL	0.3 ng/mL	[57]

Table 2. Cont.

Analyte	Components of Sandwich Assay	Method of Detection	Linear Range	Limit of Detection	Ref.
Immuno-globulin E (IgE)	Glassy carbon electrode/multi-wall carbon nanotubes + ionic liquid + chitosan composite conjugated to terephthaloyl chloride conjugated to thionine/5'-NH <sub>2</sub> -IgE aptamer/IgE/biotinylated aptamer/streptavidin-horseradish peroxidase conjugate	Differential Pulse Voltammetry	0.05–2 nM	6 pM	[58]
Glycated hemoglobin (hbA1c) and total hemoglobin (tHb)	Screen-printed gold electrode/gold nanoparticles modified with thiolated aptamer and mercaptohexanol/hbA1c or tHb	Square wave voltammetry	100 pg/mL–100 ng/mL	0.2 ng/mL (tHb); 0.34 ng/mL (hbA1c)	[59]
Prostate-specific antigen (PSA)	Screen-printed Au electrode/self-assembled monolayer/streptavidin/biotinylated aptamer/PSA/fluorescein-labeled aptamer/anti-fluorescein-peroxidase conjugate	Chrono-amperometry	Nonlinear, Langmuir fit; 0.66–25 ng/mL in diluted serum; 0.66–62.5 ng/mL in TBS buffer	0.66 ng/mL	[60]
Adenosine tri-phosphate (ATP)	Nanoporous gold on gold recordable CD/capture aptamer/ATP/diamino benzoic acid labeled detection aptamer	Differential pulse voltammetry	Nonlinear, 100 nM to 3 mM	100 nM	[62]
Cardiac troponin I (cTnI)	Screen-printed gold electrode/DNA nanotetrahedron/ aptamer/cTnI/Fe <sub>3</sub> O <sub>4</sub> nanoparticles with aptamer and horseradish peroxidase (HRP), HRP-mimicking Au@Pt nanozymes and G-quadruplex/hemin DNAzyme	Differential pulse voltammetry	10–10 <sup>5</sup> pg mL <sup>-1</sup>	7.5 pg mL <sup>-1</sup>	[63]
Cardiac troponin I (cTnI)	Gold electrode/DNA nanotetrahedron/ aptamer/cTnI/magnetic metal organic frameworks decorated with Au@Pt nanoparticles, horseradish peroxidase, G-quadruplex/hemin DNAzyme, and aptamers	Differential pulse voltammetry	10–10 <sup>5</sup> pg mL <sup>-1</sup>	5.7 pg mL <sup>-1</sup>	[64]
Cardiac troponin I (cTnI)	Screen-printed carbon electrode/carboxyethylsilanetriol-modified graphene oxide/amine-terminated aptamer/cTnI/ aptamer-horseradish peroxidase conjugate	Chrono-amperometry	Up to 1.0 µg/mL	3.4 pg/mL	[65]
Cardiac troponin I (cTnI)	Screen-printed carbon electrode/Au nanoparticles/ conducting polymer layer/Tro4 aptamer/cTnI/Tro6 aptamer conjugated to hydrazine	Chrono- amperometry	1–100 pM	1.0 pM	[66]
Human epidermal growth receptor -2 (HER2)	Thiolated DNA nanotetrahedron presenting capture aptamer/HER2/Mn <sub>3</sub> O <sub>4</sub> nanoflowers decorated by Pd@Pt nanoflowers and horseradish peroxidase/complementary signal DNA on Pd@Pt nanoflowers	Differential pulse voltammetry	0.1–100 ng/mL	0.08 ng/mL	[67]
Cocaine	Screen-printed carbon electrode/graphene and gold nanoparticles/ aptamer/cocaine/biotinylated aptamer/streptavidin-alkaline phosphatase conjugate	Differential pulse voltammetry	1–500 nM	1 nM	[68]
MCF-7 human breast cancer cells	Gold electrode/thiolated aptamer/cells/horseradish peroxidase labeled aptamer	Cyclic voltammetry	100–10 <sup>7</sup> cells	100 cells	[69]
MCF-7 human breast cancer cells	Glassy carbon electrode/multi-walled carbon nanotube and poly(glutamic acid) composite/MUC-1 aptamer/MCF-7 cell/Ag nanoparticles labeled with MUC-1 aptamer	Differential pulse voltammetry	2–7 in log(cells mL <sup>-1</sup> )	25 cells	[70]
<i>S. Aureus</i> bacteria	Streptavidin coated magnetic beads/biotinylated aptamer/bacteria/ aptamer-modified silver nanoparticles	Differential pulse voltammetry	10 to 1 × 10 <sup>6</sup> CFU/mL	1.0 CFU/mL	[71]
Vaspin	Screen-printed Au electrode/gold-sputtered coccoliths/thiolated aptamer/vaspin/ aptamer-horseradish peroxidase conjugate	Chrono-amperometry	Up to 18 nM	298 pM	[72]
Lysozyme	Gold electrode/dithiothreitol and aptamer/lysozyme/gold nanoparticle labeled with aptamer and horseradish peroxidase	Differential pulse voltammetry	Linear in log[lys] from 0.01–105 pg/mL	0.003 pg/mL	[73]



#### 4. Electrochemical Sandwich Assays Combining Aptamers and Antibodies

A number of studies have used an aptamer together with an antibody. This can be an attractive approach when there are not two aptamers available that will bind to different regions of the target to create a sandwich. There are also established schemes for use of antibodies as detection agents such as when they are labeled with enzymes. Immobilization of either aptamer or antibody on the electrode surface may be utilized. For example, a sandwich assay for the viral protein of the H5N1 avian flu virus was designed using an H5N1 aptamer and an anti-H5N1 antibody that was conjugated to alkaline phosphatase (ALP) [74]. Gold nanoparticles were formed by electrodeposition from  $\text{HAuCl}_4$  solution onto screen-printed carbon electrodes then modified with 3-mercaptopropionic acid to which the aptamer was conjugated using EDC/NHSS chemistry (NHSS = N-hydroxysulfosuccinimide). Incubation with H5N1 protein at different concentrations was done for 1 h followed by incubation with the antibody–enzyme conjugate for 1 h. The substrate p-aminophenylphosphate was converted to p-aminophenol by ALP that could be detected by its oxidation to p-quinoneimine. Detection was done using currents from cyclic voltammetry and from DPV and compared with DPV being found to be twice as sensitive. The response vs. protein concentration showed two linear regions, from 100 fM to 100 pM and from 25–100 pM. The detection limit was found to be 100 fM, comparing favorably with commercial ELISA.

A biosensor for lysozyme was developed by first covalently immobilizing a 40-mer onto screen-printed carbon electrodes [75]. Sodium nitrite ( $\text{NaNO}_2$ ) and 4-aminobenzoic acid were reacted to form a 4-diazonium cation of benzoic acid that was then reacted with the carbon surface during a linear potential sweep from 0.6 to  $-0.8$  V (vs. Ag/AgCl) to give covalently immobilized benzoic acid moieties on the carbon surface. The covalently immobilized benzoic acid was activated with EDC/NHS chemistry to covalently attach the aptamer through the 5'-end. Incubation of the lysozyme with the aptamer-modified electrode was done for 15 min, followed by incubation with the biotinylated anti-lysozyme antibody for 1 h. The next step was incubation with avidin labeled with alkaline phosphatase for 1 h. The substrate used was 1-naphthyl phosphate with product 1-naphthol detected by DPV. The parameters of detection pH (7.4), concentration of anti-lysozyme antibody, concentration of alkaline phosphatase–avidin, and lysozyme incubation time were all optimized. The detection limit achieved of 4.3 fM was the lowest reported to date, and the linear range from 1 fM–5 nM was noted as broad compared to most of those previously reported. The selectivity was tested using BSA, cytochrome c, and casein and found to be very good, as was sample recovery for lysozyme spiked into wine samples.

An aptamer sandwich-based assay was developed for protein tyrosine kinase-7 (PTK7), a biomarker for breast and possibly other cancers, using gold nanoparticle-modified screen-printed carbon electrodes (SPCE), as depicted in Figure 7 [76]. PTK7 is a type of membrane protein that plays an important role in cell recognition, ion transport as well as cancer development [77]. The gold nanoparticles were modified with mercaptopropionic acid then conjugated to the amine-terminated aptamer (5'- $\text{H}_2\text{N}$ -ATC TTA CTG CTG CGC CGC CGG GAA AAT ACT GTA CGG TTA GAT TTT TTT TTT-3') using EDC/sulfo-NHS. The gold nanoparticles were electrodeposited onto SPCE from 0.5 mM  $\text{HAuCl}_4$  in 0.5 M  $\text{H}_2\text{SO}_4$  while stirring at 0.18 V for 400 s. The sandwich structure consisted of the surface-bound aptamer, PTK7, and an anti-PTK7 antibody labeled with alkaline phosphatase. The binding of PTK7 to the surface-bound aptamer and to the anti-PTK7 antibody was evaluated on planar gold by SPR and the formation of the sandwich complex was also confirmed by SPR. The substrate used for ALP was p-aminophenylphosphate and oxidation of the product p-aminophenol was detected electrochemically using both CV and DPV in 50 mM TRIS buffer of pH 9. The current responses showed two distinct linear ranges as a function of PTK7 concentration, one from 0.1–10 pM and a second from 20–300 pM, and the limit of detection was 100 fM.

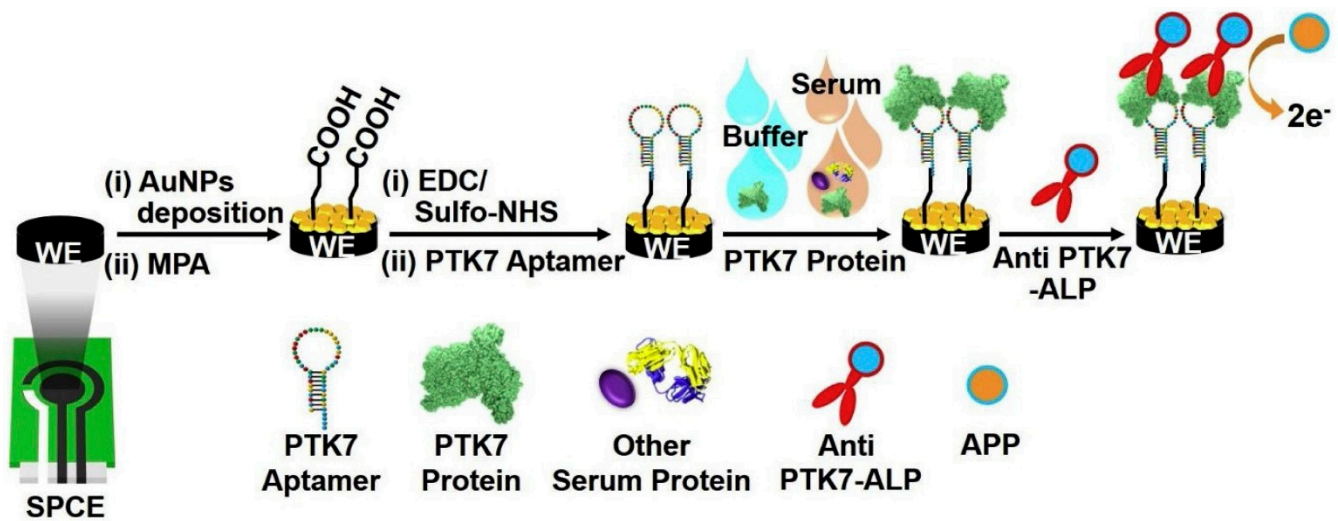


**Figure 7.** Schematic of the electrochemical sandwich assay for protein tyrosine kinase-7 that uses an aptamer and an antibody labeled with the enzyme alkaline phosphatase. Reproduced with permission from reference [76]. Copyright Elsevier 2021.

A capacitive-based aptamer-based immunosensor was developed for the detection of vascular endothelial growth factor-165 (VEGF) in human serum [78]. The aptamer-based immunosensor utilized a highly specific and selective VEGF aptamer functionalized on the aptasensor. The assay design involves capturing of VEGF protein followed by sandwiching with antibody-conjugated magnetic beads and then the change in capacitance was measured using non-faradaic electrochemical impedance spectroscopy. Interdigitated gold electrode arrays were used which were modified with mercaptopropionic acid followed by conjugation to the 5'-NH<sub>2</sub>-(CH<sub>2</sub>)<sub>6</sub>-modified aptamer using EDC/NHS chemistry. The signal generated using this aptasensor was greatly enhanced by the use of the magnetic beads with the detection range of 5 pg mL<sup>-1</sup> to 1 ng mL<sup>-1</sup> of VEGF protein in human serum achieved with no additional reagents or redox species.

The  $\beta$ -amyloid oligomers associated with Alzheimer's disease were detected by an antibody–aptamer electrochemical sandwich assay. Amyloid  $\beta$ -peptide (A $\beta$ ) in its oligomeric form is often considered as the most toxic species in Alzheimer's disease (AD) [79]. Antibodies for A $\beta$  oligomers were used as the recognition elements for specifically binding to A $\beta$  oligomers. A nanocomposite of aptamer-Au-thionine prepared by in situ modification of gold nanoparticles (AuNPs) with DNA aptamer and thionine (Th) was utilized as the detection probe. A $\beta$  oligomer-specific DNA aptamers were isolated by the combination of a gel-shift assay and a competitive screening method. The electrochemical signal was generated and amplified by high loading of Th on AuNPs, and a limit of detection of 100 pM was achieved with a linear range of 0.5–30 nM. The physiological level of A $\beta$  in normal human cerebrospinal fluid (CSF) is about 1–2 nM. The level of A $\beta$  oligomers in CSF is efficacious for predicting the severity and the progression of the early preclinical stage of the AD disease. The level of the protein tau in cerebrospinal fluid is also thought to be clinically significant for the prognosis of Alzheimer's disease and an aptamer-antibody electrochemical sandwich assay has been developed for the  $\tau$ -381 form of the protein [80]. In this assay, an Au electrode was modified by mercaptopropionic acid and the anti-tau antibody was linked to the surface using EDC/NHS chemistry. Au nanoparticles were modified with cysteamine and the tau aptamer of the sequence 5'-H<sub>2</sub>N-GCGGAGCGTGGCAGG-3'. Differential pulse voltammetry was used with [Fe(CN)<sub>6</sub>]<sup>3-/4-</sup> used as a redox probe. A current response linear in log[tau] was found for the concentrations studied ranging from 0.5–100 pM  $\tau$ -381 in 0.1 M PBS. Recovery in the detection of  $\tau$ -381 from human cerebrospinal fluid samples diluted 100-fold in 0.1 M PBS was found to be excellent.

Human immunoglobulin E (IgE) was detected by using methylene blue (MB) as a redox probe and using the combined advantages of the aptamer, nanomaterial and antibody to design the electrochemical sandwich biosensor [81]. Goat anti-human IgE was immobilized on the surface of the gold electrode followed by exposure to different concentrations of human IgE. The aptamer immobilized Au NPs can bind with human IgE at different binding sites and this specific binding of the aptamer and human IgE on the electrode surface enables the accumulation of the MB on the electrode surface by the interaction of MB with G bases in the aptamer and therefore an amplified signal was observed in the electrochemical sensing system. The range of the detection of human IgE was 1–10,000 ng mL<sup>-1</sup> with a limit of detection of 0.52 ng mL<sup>-1</sup>.

C-reactive protein (CRP) is one of the cytokine-induced acute phase proteins and its normal concentration in serum is below 5.0 mg L<sup>-1</sup> with a clinical range within 1–500 mg L<sup>-1</sup>, and is widely accepted as one of the biomarkers for cardiovascular diseases and inflammation. An RNA aptamer-based electrochemical aptasensor was designed to detect C-reactive protein using functionalized silica microspheres as immunoprobes, and is depicted in Figure 8 [82]. Silica microspheres were synthesized and then functionalized with Au nanoparticles to provide a large surface area for immobilizing Zn<sup>2+</sup> and antibodies. The CRP aptamer used was a 44-mer RNA aptamer of sequence: 5'-SH-(CH<sub>2</sub>)<sub>6</sub>-GCCUGUAAGGUGGUCGGUGUGGGGAGUGUGUUAGGAGAGAUUGC-3'. The aptamer was immobilized on the surface of Au nanoparticles deposited onto GCE for 5 h. An immunoprobe was prepared by the incubation of the anti-CRP (Ab) on the AuNP-modified silica microspheres followed by re-dispersion in a solution of Zn(NO<sub>3</sub>)<sub>2</sub> to load the Zn<sup>2+</sup> on the surface. Various concentrations of the CRP samples were sandwiched between the aptamer immobilized electrode and immunoprobe and the response was recorded by SWV detecting reduction of Zn<sup>2+</sup>. Under optimized conditions, the linear range of the detection was 0.005–125 ng mL<sup>-1</sup>, and the detection limit was 0.0017 ng mL<sup>-1</sup>.

An electrochemical aptamer–antibody sandwich assay for CRP was developed with the aid of magnetic nanoparticles [83]. Streptavidin-coated magnetic beads (1.05 μm size) were modified with a CRP 44-mer RNA aptamer that was 5'-biotinylated. The incubation period was 15 min followed by washing for 2 min which was aided by collecting the particles using a magnetic field and then re-suspending them. After binding of CRP, a biotinylated monoclonal antibody to CRP was then bound, again for 15 min followed by a magnetically aided washing step. Finally, a conjugate of streptavidin and alkaline phosphatase was added and after washing the particles were magnetically collected onto SPCE. Using the substrate 1-naphthylphosphate and DPV detection of the 1-naphthol product a dose–response curve was obtained with a measuring range of 1–1000 mg L<sup>-1</sup>, a dynamic range from 0.1–50 mg L<sup>-1</sup> and a limit of detection of 0.054 mg L<sup>-1</sup>.

An aptamer–antibody sandwich assay was developed for α-1 antitrypsin (AAT), a biomarker for Alzheimer's disease [84]. Carbon nanotubes (1–5 μm, d~20 nm) were modified by adsorption of 3, 4, 9, 10-perylene tetracarboxylic acid and then cast onto screen-printed carbon electrodes (SPCE). The carboxylic groups were then activated by EDC/NHS chemistry and conjugated to the 37-mer AAT aptamer. The other part of the sandwich was composed of silver nanoparticles that were modified by mercaptopropionic acid followed by application of EDC/NHS chemistry and conjugation to an anti-AAT monoclonal antibody conjugated to alkaline phosphatase. Incubation of the aptamer-modified electrode with AAT was for 1 h and detection was done using DPV with p-aminophenylphosphate (p-APP) at 100 μM as higher p-APP concentration did not increase the response further. A linear range from 0.05–20 pM was found with a detection limit of 0.01 pM. The assay was found to be selective against IgG or IgE interfering proteins, and recovery from serum samples with AAT was 95–102%.

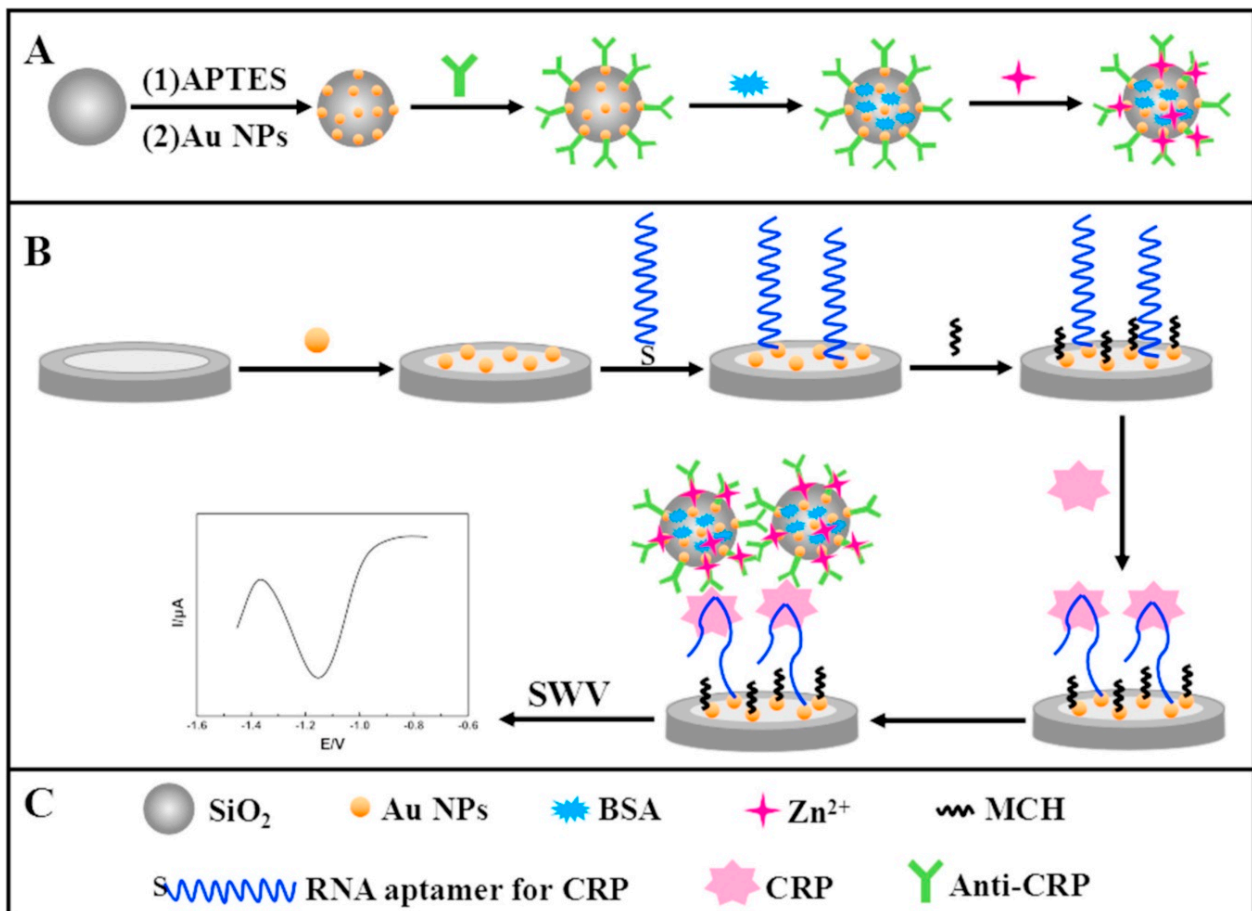


**Figure 8.** Schematic representation of fabrication process of the CRP aptasensor. (A) Preparation of immunoprobe  $Zn^{2+}/Ab/Au$  NPs@Si MSs, (B) Fabrication of MCH/RNA/Au NP-modified electrode. (C) Depiction of the components of the CRP aptasensor. Reprinted with permission from reference [82]. Copyright Elsevier 2017.

An antibody–aptamer sandwich assay for a platelet-derived growth factor (PDGF) was developed using a circular DNA probe for signal enhancement [85]. A gold electrode ( $d = 3$  mm) was modified by mercaptopropionic acid and rabbit anti-human IgG for PDGF was conjugated to the surface using EDC/NHS chemistry followed by blocking of the remaining surface using bovine serum albumin (BSA). An aptamer binding PDGF was extended by a circular DNA probe then hybridized using DNA polymerase. The completion of the sandwich by binding of the aptamer–circular DNA probe was detected by binding of methylene blue whose reduction was detected by SWV. A linear range from  $50$ – $500$   $ng\ mL^{-1}$  and a detection limit of  $18$   $pg\ mL^{-1}$  were found, and agreement of the assay with traditional ELISA was excellent.

Another antibody–aptamer sandwich assay was designed for the cancer biomarker MUC1 [86]. Screen-printed electrodes with a graphite working electrode were used as a substrate on which to electropolymerize *o*-aminobenzoic acid. The conducting polymer was then conjugated to a primary antibody against MUC1 using EDC/NHS chemistry with unreacted sites capped using ethanolamine. An aptamer binding to another site on MUC1 completed the sandwich and binding of methylene blue was detected by its reduction during a DPV sweep. The binding of MUC1 to antibody was done for 90 min and the binding to aptamer was allowed to take place overnight. An increase in charge transfer resistance during each step of immobilization and sandwich formation was seen clearly using electrochemical impedance spectroscopy. A linear range of 3–10 ppb with a detection limit of 2.4 ppb was obtained. A related electrochemical sensor was developed for the detection of cancer biomarker glycoprotein MUC16 using indium tin oxide (ITO) electrodes



onto which Au nanoparticles had been electrodeposited [87]. In this approach, the MUC16 polyclonal antibody was drop-cast onto the electrode surfaces. After binding of MUC16, an aptamer with a primer tail bound to complete the sandwich. Using two DNA probes, the hybridization chain reaction was used in multiple cycles to extend the DNA strand to yield long concatamers so that more of the methylene blue redox indicator could binding to the structure. Using DPV, a linear range of 0.39–200 units mL<sup>-1</sup> with a detection limit of 0.02 units mL<sup>-1</sup> was obtained.

The inflammation marker tumor necrosis factor-alpha (TNF- $\alpha$ ) was detected using an electrochemical sandwich assay involving an aptamer and an antibody conjugated to HRP [88]. The electrode, a graphite screen-printed electrode, was covered by a film of cobalt hexacyanoferrate electrosynthesized from a solution of CoCl<sub>2</sub> and K<sub>3</sub>[Fe(CN)<sub>6</sub>] intended to provide superior electron transfer ability. Au nanoparticles (d = 15 nm) were adsorbed onto the thin film and then modified by a thiolated aptamer. After binding to TNF- $\alpha$  for 20 min, the binding of an antibody conjugated to HRP for 60 min took place. The HRP activity against the substrate o-aminophenol in H<sub>2</sub>O<sub>2</sub> was detected using DPV yielding a linear range from 1–100 ng L<sup>-1</sup> with a detection limit of 0.52 ng L<sup>-1</sup>. The step-by-step formation of the modified electrode and sandwich structure was followed by EIS. Agreement for TNF- $\alpha$  three human serum samples with results from ELISA within error bars was found.

Insulin-like growth factor 1 (IGF1) is a 70 amino acid hormone similar in structure to insulin and found to be a biomarker for abdominal aortic aneurysm. A sandwich assay on interdigitated electrodes (IDE) for IGF1 was created using a biotinylated aptamer for capture and an anti-IGF1 antibody [89]. The protein streptavidin was first bound to the IDE using 1,1-carbonyldiimidazole and then used to capture the biotinylated aptamer. The binding of IGF1 would result in a current increase upon a voltage sweep from 0–2 V across the 10  $\mu$ m IDE gaps. A detection limit of 10 fM was found and the formation of the sandwich structure was seen to increase the current levels. This sensor design involved a sandwich structure and electrodes but is not an actual electrochemical sensor.

A summary of the results from these electrochemical assays using aptamers together with antibodies is presented in Table 3.

**Table 3.** Electrochemical Sandwich Assays Combining Aptamers and Antibodies.

Analyte	Components of Sandwich Assay	Method of Detection	Linear Range	Limit of Detection	Ref.
H5N1 avian influenza virus protein	Screen-printed carbon electrode/Au nanoparticles/aptamer/H5N1/antibody–alkaline phosphatase conjugate	Differential pulse voltammetry	100 fM–10 pM and 25–100 pM	100 fM	[74]
Lysozyme	Screen-printed carbon electrode/benzoic acid/aptamer/lysozyme/biotinylated antibody/alkaline phosphatase–avidin conjugate	Differential pulse voltammetry	1 fM–5 nM	4.3 fM	[75]
Protein tyrosine kinase-7 (PTK7)	Screen-printed electrodes/Au nanoparticles/aptamer/PTK7/antibody labeled with alkaline phosphatase	Differential pulse voltammetry	100 fM–10 pM	100 fM	[76]
Vascular endothelial growth factor-165 (VEGF)	Interdigitated gold electrodes/aptamer and thionine/VEGF/antibody–conjugated magnetic beads	Non-Faradaic impedance spectroscopy	5 pg/mL–1 ng/mL	5 pg/mL	[78]
Amyloid $\beta$ -oligomers	Glassy carbon electrode/aptamer/amyloid $\beta$ /aptamer and thionine-modified Au nanoparticles	Differential pulse voltammetry	0.5–30 nM	100 pM	[79]
Tau-381 protein	Au electrode/mercaptopyronic acid monolayer/anti-tau antibody/tau-381/Au nanoparticles with aptamer and cysteamine, Fe(CN) <sub>6</sub> <sup>3-/4-</sup> in solution.	Differential pulse voltammetry	0.5–100 pM	0.5 pM	[80]
Human immunoglobulin E (IgE)	Gold electrode/antibody/aptamer-modified Au nanoparticles with methylene blue	Differential pulse voltammetry	1–10,000 ng/mL	0.52 ng/mL	[81]
C-reactive protein	Glassy carbon electrode/Au nanoparticles/aptamer/silica microspheres with Au nanoparticles and Zn <sup>2+</sup>	Square-wave voltammetry	0.005 ng/mL–125 ng/mL	0.0017 ng/mL	[82]

Table 3. Cont.

Analyte	Components of Sandwich Assay	Method of Detection	Linear Range	Limit of Detection	Ref.
C-reactive protein	Magnet/carbon electrode/streptavidin-coated magnetic beads/biotinylated aptamer/CRP/biotinylated antibody/alkaline phosphatase-streptavidin conjugate	Differential pulse voltammetry	0.1–50 mg/L (nonlinear response)	0.054 mg/L	[83]
$\alpha$ -1 antitrypsin (AAT)	Screen-printed electrode/carbon nanotubes/aptamer/AAT/Ag nanoparticles modified by antibody-alkaline phosphatase conjugate	Differential pulse voltammetry	0.05–20 pM	0.01 pM	[84]
Platelet-derived growth factor BB (PDGF-BB)	Gold electrode/antibody/PDGF/aptamer with circular DNA probe/methylene blue	Square-wave voltammetry	50–500 ng mL <sup>-1</sup>	18 pg mL <sup>-1</sup>	[85]
Mucin protein-1 (MUC1)	Graphite working electrode/conducting polymer/antibody/MUC1/aptamer/methylene blue	Differential pulse voltammetry	3–10 ppb	2.4 ppb	[86]
Mucin protein-16 (MUC16)	Indium tin oxide electrode/gold nanoparticles/antibody/MUC16/aptamer and primer tail/DNA/methylene blue	Differential pulse voltammetry	0.39–200 unit/mL	0.02 unit/mL	[87]
Tumor necrosis factor $\alpha$ (TNF $\alpha$ )	Screen-printed graphite electrode/cobalt hexacyanoferrate/Au nanoparticles/aptamer/TNF $\alpha$ /antibody conjugated to horseradish peroxidase	Differential pulse voltammetry	1–100 pg/mL	0.52 pg/mL	[88]
Insulin-like growth factor (IGF1)	Interdigitated electrode/streptavidin/biotinylated aptamer/antibody	Amperometry	10 fM–1 nM	10 fM	[89]

### 5. Electrochemical Sandwich Assay Combining Aptamers with Other Materials

Another avenue for the use of aptamers in electrochemical sandwich assays involves using other materials and molecules such as molecularly imprinted polymers, other biomolecules such as lectins, or redox-active nanomaterials. A summary of these assays is presented in Table 4. An electrochemical biosensor for the reliable detection of the amyloid- $\beta$  oligomers was developed by using molecularly imprinted polymers (MIPs) and aptamer as the recognition element by forming an MIPs/target/aptamer sandwich assay [90] as shown in Figure 9. The A $\beta$ -specific aptamer was immobilized on the surface of 200 nm SiO<sub>2</sub> nanoparticles decorated by a shell of smaller Ag nanoparticles using HS-aptamer via Ag-S bonds to yield the SiO<sub>2</sub>@Ag-aptamer bioconjugate. An MIP biosensor for A $\beta$ <sub>1–42</sub> was prepared by using a template of chitosan on a glassy carbon electrode onto which AuNPs and reduced graphene oxide had been deposited. Graphene oxide (GO) and gold nanoparticles (AuNPs) were used to improve the electrical conductivity and surface-to-volume ratio. Differential pulse voltammetry was used to detect the oxidation of the Ag nanoparticles. The LOD for A $\beta$ <sub>1–42</sub> oligomers was 1.22 pg mL<sup>-1</sup> with the linear range of detection 5 pg mL<sup>-1</sup> to 10 ng mL<sup>-1</sup>. The detection range of this biosensor covers much of the physiological concentration range for A $\beta$  oligomers in patients, which has been reported to be in the range of 1.25–12.5 ng mL<sup>-1</sup>.

Lectins used along with DNA aptamers have been explored as molecular recognition elements for glycoproteins. A biosensor for carcinoembryonic antigen (CEA) was developed based on Concanavalin A (Con A) and a DNA aptamer. CEA was detected with a linear range of 5–40 ng mL<sup>-1</sup> and with a limit of detection of 3.4 ng mL<sup>-1</sup>, lower than the threshold level in human serum for cancer patients of 10 ng mL<sup>-1</sup> [91]. The CEA target was selectively captured on the gold electrode surface by DNA aptamers. Con A served as the bridge between CEA and HRP (as an enzyme label) as the affinity of ConA was verified with both CEA and HRP, as both are glycoproteins. Differential pulse voltammetry (DPV) currents were measured in the presence of hydroquinone and hydrogen peroxide.

**Table 4.** Electrochemical Sandwich Assays Combining Aptamers and Lectins or Other Materials.

Analyte	Components of Sandwich Assay	Method of Detection	Linear Range	Limit of Detection	Ref.
Amyloid $\beta_{1-42}$ oligomers	Glassy carbon electrode/Graphene oxide and Au nanoparticles/Chitosan and molecularly imprinted polymer layer/A $\beta$ oligomer/aptamer-modified Ag nanoparticles bound to SiO <sub>2</sub> larger nanoparticle	Differential pulse voltammetry	5 pg/mL–10 ng/mL	1.22 pg/mL	[90]
Carcino-embryonic antigen	Au electrode/thiolated aptamer/CEA/Concanavalin A lectin/horseadish peroxidase	Differential pulse voltammetry	5–40 ng/mL	3.4 pg/mL	[91]
human epidermal growth factor receptor-2	Au electrode/HER2 specific peptide/HER2/MnO <sub>2</sub> nanosheet with phosphate ions and aptamers, molybdate ions	Square-wave voltammetry	5 pg/mL–1 ng/mL	0.05 pg/mL	[92]

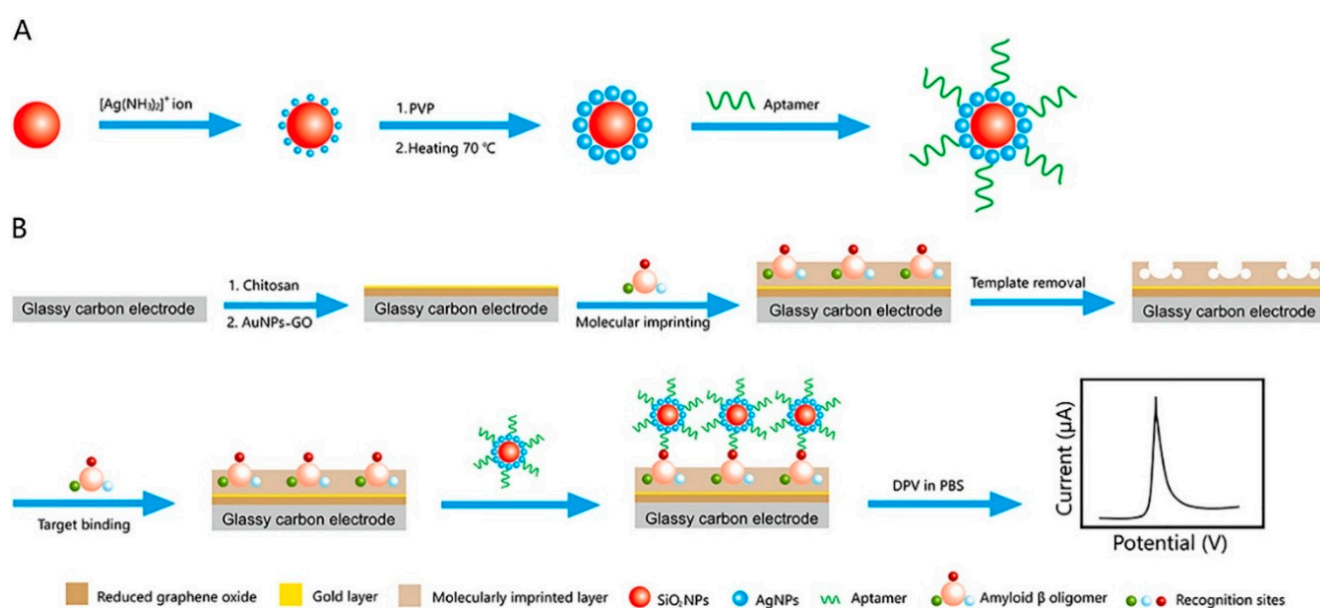


**Figure 9.** Schematic illustration of (A) the preparation of the SiO<sub>2</sub>@Ag-aptamer composite, and (B) the fabrication of the MIPs-based antibody-free biosensor and the electrochemical detection of A $\beta$  oligomer via a sandwich-type assay. Reprinted with permission from reference [90]. Copyright 2020, Elsevier.

Breast cancer biomarker human epidermal growth factor receptor-2 (HER2) was detected by aptamer-based biosensor using phosphate-functionalized MnO<sub>2</sub> nanosheets as the electrochemical probe [92]. MnO<sub>2</sub> nanosheets were synthesized and phosphate ions and the aptamer (5'-GCAGGGGTGTGGG-3') were absorbed onto the nanosheets. The reaction of phosphate ion with molybdate ion formed redox-active molybdophosphate as a precipitate on the electrode surface that was then detected using square wave voltammetry. The peptide specific to HER2 (CKLRLEWNR) was immobilized onto the gold surface followed by the different concentrations of HER2 solution. Then, a modified MnO<sub>2</sub> nanosheet was added to the modified electrode with Na<sub>2</sub>MoO<sub>4</sub> solution and current arising from reduction of molybdophosphate was measured. This assay achieved a linear range of 0.1–500 pg mL<sup>-1</sup>, and the detection limit was as low as 0.05 pg mL<sup>-1</sup>. This assay was also used to detect HER2 in spiked human serum samples giving good agreement with ELISA results.

## 6. Discussion

In recent years, a number of important trends have emerged in the development of electrochemical sandwich assays using aptamers. Given that many biomarker proteins are glycoproteins, the development of a pair of aptamers where the binding of one member

of the pair depends on the glycosylation state of the protein is important since abnormal glycosylation is found in many disease states [93]. Given the significance of glycoproteins as assay targets, the incorporation of lectins with aptamers in sandwich assays is likely to develop further. A trend toward more sophisticated architecture making use of a wider variety of nanomaterials is evident in recent years. Within the past five years, the use of carbon nanotubes in assay structures has increased, and highly novel structures such as gold-sputtered coccoliths [72], doped graphene oxide nanosheets [48], hollow CeO<sub>2</sub> particles [54], Mn<sub>3</sub>O<sub>4</sub> and Pd@Pt nanozymes [67], and MnO<sub>2</sub> nanosheets [92] have been introduced. These nanomaterials are used as supports for the detection of aptamers or antibodies and also for signal-producing enzymes with the goal of increasing sensitivity and dynamic range. These materials can also in some cases exhibit improved electron transfer behavior. While sandwich assays for thrombin continue to be explored, efforts are diversifying to a wide range of other biomarkers and targets of diagnostic significance. The development of additional complimentary aptamer pairs that bind to distinct regions of a protein target will be important for the advancement of these assays.

Aptamers have proven to be a highly valuable tool for the development of electrochemical assays. The stability of aptamers and their ability to regenerate into their active conformations makes their use in assays especially robust. Aptamers can be used to modify nanoparticles and nanomaterials employed for assay signal amplification. Aptamers also open the possibility for amplification by applying processes that extend the length of the DNA associated with detection for binding of a greater number of redox markers when detection takes place using chronocoulometry. Common nanoparticles such as gold nanoparticles are popular choices for signal amplification but other more unique nanomaterials such as nanodiamonds, templated materials, nanocages and others have proven well worthy of investigation.

For these electrochemical sandwich assays, differential pulse voltammetry which provides reduced background current from double-layer charging and its sensitivity stands out as a method of choice. Other electrochemical methods such as cyclic voltammetry and electrochemical impedance spectroscopy are useful for the characterization of the electrode assembly and stepwise modification. While those assays whose current response is linear in analyte concentration are most convenient, those that are linear in the logarithm of the analyte concentration or exhibiting a nonlinear dose–response curve are also useful. It is important for those researchers developing electrochemical sandwich assays using aptamers to be cognizant of the relevant and useful range for the specific analyte being examined. The achievement of lower detection limits provides the opportunity to dilute real clinical samples and thereby limit matrix effects. Further demonstration of the value of this approach to testing real clinical samples is an important objective for some of these assays to achieve regular and practical use. The potential convenience and low cost of electrochemical methods make the further development and refinement of electrochemical sandwich assays including aptamers promising areas for continued development.

**Funding:** This research received no external funding.

**Conflicts of Interest:** The author declares no conflict of interest.

## References

1. Ziółkowski, R.; Jarczewska, M.; Górski, L.; Malinowska, E. From Small Molecules toward Whole Cells Detection: Application of Electrochemical Aptasensors in Modern Medical Diagnostics. *Sensors* **2021**, *21*, 724. [[CrossRef](#)] [[PubMed](#)]
2. Seo, H.B.; Gu, M.B. Aptamer-based sandwich-type biosensors. *J. Biol. Eng.* **2017**, *11*, 11. [[CrossRef](#)] [[PubMed](#)]
3. Yáñez-Sedeño, P.; Campuzano, S.; Pingarrón, J. Pushing the limits of electrochemistry toward challenging applications in clinical diagnosis, prognosis, and therapeutic action. *Chem. Commun.* **2019**, *55*, 2563–2592. [[CrossRef](#)]
4. Rusling, J.F. Multiplexed electrochemical protein detection and translation to personalized cancer diagnostics. *Anal. Chem.* **2013**, *85*, 5304–5310. [[CrossRef](#)]
5. Lin, Y.-Y.; Wang, J.; Liu, G.; Wu, H.; Wai, C.M.; Lin, Y. A nanoparticle label/immunochromatographic electrochemical biosensor for rapid and sensitive detection of prostate-specific antigen. *Biosens. Bioelectron.* **2008**, *23*, 1659–1665. [[CrossRef](#)] [[PubMed](#)]



6. Khoshroo, A.; Mazloum-Ardakani, M.; Forat-Yazdi, M. Enhanced performance of label-free electrochemical immunosensor for carbohydrate antigen 15-3 based on catalytic activity of cobalt sulfide/graphene nanocomposite. *Sens. Actuat. B Chem.* **2018**, *255*, 580–587. [[CrossRef](#)]
7. Chikkaveeraiah, B.V.; Bhirde, A.A.; Morgan, N.Y.; Eden, H.S.; Chen, X. Electrochemical Immunosensors for Detection of Cancer Protein Biomarkers. *ACS Nano* **2012**, *6*, 6546–6561. [[CrossRef](#)] [[PubMed](#)]
8. Song, S.; Wang, L.; Li, J.; Fan, C.; Zhao, J. Aptamer-based biosensors. *TrAC Trends Anal. Chem.* **2008**, *27*, 108–117. [[CrossRef](#)]
9. Huang, Y.; Xu, J.; Liu, J.; Wang, X.; Chen, B. Disease-related detection with electrochemical biosensors: A review. *Sensors* **2017**, *17*, 2375. [[CrossRef](#)] [[PubMed](#)]
10. Hianik, T.; Wang, J. Electrochemical Aptasensors—Recent Achievements and Perspectives. *Electroanal. Int. J. Devoted Fundam. Pract. Asp. Electroanal.* **2009**, *21*, 1223–1235. [[CrossRef](#)]
11. Cox, J.C.; Ellington, A.D. Automated selection of anti-protein aptamers. *Bioorg. Med. Chem.* **2001**, *9*, 2525–2531. [[CrossRef](#)]
12. Stoltenburg, R.; Nikolaus, N.; Strehlitz, B. Capture-SELEX: Selection of DNA aptamers for aminoglycoside antibiotics. *J. Anal. Methods Chem.* **2012**, *415697*, 1–14. [[CrossRef](#)]
13. Jayasena, S.D. Aptamers: An emerging class of molecules that rival antibodies in diagnostics. *Clin. Chem.* **1999**, *45*, 1628–1650. [[CrossRef](#)]
14. Sun, H.; Zu, Y. A highlight of recent advances in aptamer technology and its application. *Molecules* **2015**, *20*, 11959–11980. [[CrossRef](#)] [[PubMed](#)]
15. Fang, X.; Tan, W. Aptamers generated from cell-SELEX for molecular medicine: A chemical biology approach. *Acc. Chem. Res.* **2010**, *43*, 48–57. [[CrossRef](#)]
16. De Girolamo, A.; McKeague, M.; Pascale, M.; Cortese, M.; DeRosa, M.C. Immobilization of Aptamers on Substrates. In *Aptamers for Analytical Applications: Affinity Acquisition and Method Design*; Dong, Y., Ed.; Wiley: New York, NY, USA, 2018; pp. 85–126.
17. Meini, N.; Farre, C.; Chaix, C.; Kherrat, R.; Dzyadevych, S.; Jaffrezic-Renault, N. A sensitive and selective thrombin impedimetric aptasensor based on tailored aptamers obtained by solid-phase synthesis. *Sens. Actuat. B Chem.* **2012**, *166*, 715–720. [[CrossRef](#)]
18. Jolly, P.; Batistuti, M.R.; Ustuner, S.; Mulato, M.; Arya, S.K.; Estrela, P. Nucleic Acid-Based Aptasensors for Cancer Diagnostics: An Insight into Immobilisation Strategies. In *Next Generation Point-of-Care Biomedical Sensors Technologies for Cancer Diagnosis*; Chandra, P., Tan, Y.N., Singh, S., Eds.; Springer: New York, NY, USA, 2017; pp. 205–231.
19. Li, X.; Shen, L.; Zhang, D.; Qi, H.; Gao, Q.; Ma, F.; Zhang, C. Electrochemical impedance spectroscopy for study of aptamer-thrombin interfacial interactions. *Biosens. Bioelectron.* **2008**, *23*, 1624–1630. [[CrossRef](#)]
20. Tabrizi, M.A.; Shamsipur, M.; Saber, R.; Sarkar, S.; Sherkatkhameneh, N. Flow injection amperometric sandwich-type electrochemical aptasensor for the determination of adenocarcinoma gastric cancer cell using aptamer-Au@ Ag nanoparticles as labeled aptamer. *Electrochim. Acta* **2017**, *246*, 1147–1154. [[CrossRef](#)]
21. Chen, D.; Feng, H.; Li, J. Graphene oxide: Preparation, functionalization, and electrochemical applications. *Chem. Rev.* **2012**, *112*, 6027–6053. [[CrossRef](#)] [[PubMed](#)]
22. Hayat, A.; Sassolas, A.; Marty, J.-L.; Radi, A.-E. Highly sensitive ochratoxin A impedimetric aptasensor based on the immobilization of azido-aptamer onto electrografted binary film via click chemistry. *Talanta* **2013**, *103*, 14–19. [[CrossRef](#)] [[PubMed](#)]
23. Balamurugan, S.; Obubuafo, A.; Soper, S.A.; Spivak, D.A. Surface immobilization methods for aptamer diagnostic applications. *Anal. Bioanal. Chem.* **2008**, *390*, 1009–1021. [[CrossRef](#)]
24. Di Cera, E. Thrombin. *Mol. Asp. Med.* **2008**, *29*, 203–254. [[CrossRef](#)] [[PubMed](#)]
25. Ireson, C.R.; Kelland, L.R. Discovery and development of anticancer aptamers. *Mol. Cancer Ther.* **2006**, *5*, 2957–2962. [[CrossRef](#)]
26. Padmanabhan, K.; Padmanabhan, K.; Ferrara, J.; Sadler, J.E.; Tulinsky, A. The structure of alpha-thrombin inhibited by a 15-mer single-stranded DNA aptamer. *J. Biol. Chem.* **1993**, *268*, 17651–17654. [[CrossRef](#)]
27. Li, Y.; Guo, L.; Zhang, F.; Zhang, Z.; Tang, J.; Xie, J. High-sensitive determination of human  $\alpha$ -thrombin by its 29-mer aptamer in affinity probe capillary electrophoresis. *Electrophoresis* **2008**, *29*, 2570–2577. [[CrossRef](#)] [[PubMed](#)]
28. Lin, P.-H.; Chen, R.-H.; Lee, C.-H.; Chang, Y.; Chen, C.-S.; Chen, W.-Y. Studies of the binding mechanism between aptamers and thrombin by circular dichroism, surface plasmon resonance and isothermal titration calorimetry. *Coll. Surf. B* **2011**, *88*, 552–558. [[CrossRef](#)] [[PubMed](#)]
29. Trapaidze, A.; Héroult, J.-P.; Herbert, J.-M.; Bancaud, A.; Gué, A.-M. Investigation of the selectivity of thrombin-binding aptamers for thrombin titration in murine plasma. *Biosens. Bioelectron.* **2016**, *78*, 58–66. [[CrossRef](#)]
30. Deng, B.; Lin, Y.; Wang, C.; Li, F.; Wang, Z.; Zhang, H.; Li, X.-F.; Le, X.C. Aptamer binding assays for proteins: The thrombin example—A review. *Anal. Chim. Acta* **2014**, *837*, 1–15. [[CrossRef](#)] [[PubMed](#)]
31. Li, J.; Hu, X.; Shi, S.; Zhang, Y.; Yao, T. Three label-free thrombin aptasensors based on aptamers and  $[Ru(bpy)_2(o-mopip)]^{2+}$ . *J. Mater. Chem. B* **2016**, *4*, 1361–1367. [[CrossRef](#)]
32. Crawley, J.; Zanardelli, S.; Chion, C.; Lane, D. The central role of thrombin in hemostasis. *J. Thromb. Haemost.* **2007**, *5*, 95–101. [[CrossRef](#)]
33. Huntington, J.A. How  $Na^+$  activates thrombin—a review of the functional and structural data. *Biol. Chem.* **2008**, *389*, 1025–1035. [[CrossRef](#)] [[PubMed](#)]
34. Lee, M.; Walt, D.R. A fiber-optic microarray biosensor using aptamers as receptors. *Anal. Biochem.* **2000**, *282*, 142–146. [[CrossRef](#)]
35. Xiao, Y.; Lubin, A.A.; Heeger, A.J.; Plaxco, K.W. Label-Free Electronic Detection of Thrombin in Blood Serum by Using an Aptamer-Based Sensor. *Angew. Chem.* **2005**, *44*, 5456–5459. [[CrossRef](#)]

36. Lin, S.-F.; Ding, T.-J.; Liu, J.-T.; Lee, C.-C.; Yang, T.-H.; Chen, W.-Y.; Chang, J.-Y. A guided mode resonance aptasensor for thrombin detection. *Sensors* **2011**, *11*, 8953–8965. [[CrossRef](#)]
37. Baek, S.H.; Wark, A.W.; Lee, H.J. Dual nanoparticle amplified surface plasmon resonance detection of thrombin at subattomolar concentrations. *Anal. Chem.* **2014**, *86*, 9824–9829. [[CrossRef](#)]
38. Li, B.; Wang, Y.; Wei, H.; Dong, S. Amplified electrochemical aptasensor taking AuNPs based sandwich sensing platform as a model. *Biosens. Bioelectron.* **2008**, *23*, 965–970. [[CrossRef](#)]
39. Ikebukuro, K.; Kiyohara, C.; Sode, K. Electrochemical Detection of Protein Using a Double Aptamer Sandwich. *Anal. Lett.* **2004**, *37*, 2901–2909. [[CrossRef](#)]
40. Numnuam, A.; Chumbimuni-Torres, K.Y.; Xiang, Y.; Bash, R.; Thavarungkul, P.; Kanatharana, P.; Pretsch, E.; Wang, J.; Bakker, E. Aptamer-Based Potentiometric Measurements of Proteins Using Ion-Selective Microelectrodes. *Anal. Chem.* **2008**, *80*, 707–712. [[CrossRef](#)]
41. Wang, Q.; Zhou, Z.; Zhai, Y.; Zhang, L.; Hong, W.; Zhang, Z.; Dong, S. Label-free aptamer biosensor for thrombin detection based on functionalized graphene nanocomposites. *Talanta* **2015**, *141*, 247–252. [[CrossRef](#)]
42. Qiu, H.; Sun, Y.; Huang, X.; Qu, Y. A sensitive nanoporous gold-based electrochemical aptasensor for thrombin detection. *Coll. Surf. B* **2010**, *79*, 304–308. [[CrossRef](#)] [[PubMed](#)]
43. Hu, J.; Wang, T.; Kim, J.; Shannon, C.; Easley, C.J. Quantitation of Femtomolar Protein Levels via Direct Readout with the Electrochemical Proximity Assay. *J. Am. Chem. Soc.* **2012**, *134*, 7066–7072. [[CrossRef](#)]
44. Centi, S.; Tombelli, S.; Minunni, M.; Mascini, M. Aptamer-Based Detection of Plasma Proteins by an Electrochemical Assay Coupled to Magnetic Beads. *Anal. Chem.* **2007**, *79*, 1466–1473. [[CrossRef](#)]
45. Centi, S.; Messina, G.; Tombelli, S.; Palchetti, I.; Mascini, M. Different approaches for the detection of thrombin by an electrochemical aptamer-based assay coupled to magnetic beads. *Biosens. Bioelectron.* **2008**, *23*, 1602–1609. [[CrossRef](#)]
46. Ding, C.; Ge, Y.; Lin, J.-M. Aptamer based electrochemical assay for the determination of thrombin by using the amplification of the nanoparticles. *Biosens. Bioelectron.* **2010**, *25*, 1290–1294. [[CrossRef](#)]
47. Gao, F.; Du, L.; Zhang, Y.; Zhou, F.; Tang, D. A sensitive sandwich-type electrochemical aptasensor for thrombin detection based on platinum nanoparticles decorated carbon nanocages as signal labels. *Biosens. Bioelectron.* **2016**, *86*, 185–193. [[CrossRef](#)]
48. He, B. Sandwich electrochemical thrombin assay using a glassy carbon electrode modified with nitrogen-and sulfur-doped graphene oxide and gold nanoparticles. *Microchim. Acta* **2018**, *185*, 344. [[CrossRef](#)]
49. Ikebukuro, K.; Kiyohara, C.; Sode, K. Novel electrochemical sensor system for protein using the aptamers in sandwich manner. *Biosens. Bioelectron.* **2005**, *20*, 2168–2172. [[CrossRef](#)]
50. Kang, Y.; Feng, K.-J.; Chen, J.-W.; Jiang, J.-H.; Shen, G.-L.; Yu, R.-Q. Electrochemical detection of thrombin by sandwich approach using antibody and aptamer. *Bioelectrochemistry* **2008**, *73*, 76–81. [[CrossRef](#)]
51. Yeh, F.-Y.; Liu, T.-Y.; Tseng, I.-H.; Yang, C.-W.; Lu, L.-C.; Lin, C.-S. Gold nanoparticles conjugates-amplified aptamer immunosensing screen-printed carbon electrode strips for thrombin detection. *Biosens. Bioelectron.* **2014**, *61*, 336–343. [[CrossRef](#)]
52. Zhao, J.; Zhang, Y.; Li, H.; Wen, Y.; Fan, X.; Lin, F.; Tan, L.; Yao, S. Ultrasensitive electrochemical aptasensor for thrombin based on the amplification of aptamer-AuNPs-HRP conjugates. *Biosens. Bioelectron.* **2011**, *26*, 2297–2303. [[CrossRef](#)]
53. Chung, S.; Moon, J.-M.; Choi, J.; Hwang, H.; Shim, Y.-B. Magnetic force assisted electrochemical sensor for the detection of thrombin with aptamer-antibody sandwich formation. *Biosens. Bioelectron.* **2018**, *117*, 480–486. [[CrossRef](#)] [[PubMed](#)]
54. Zhang, Q.; Fan, G.; Chen, W.; Liu, Q.; Zhang, X.; Zhang, X.; Liu, Q. Electrochemical sandwich-type thrombin aptasensor based on dual signal amplification strategy of silver nanowires and hollow Au-CeO<sub>2</sub>. *Biosens. Bioelectron.* **2020**, *150*, 111846. [[CrossRef](#)]
55. Fang, L.-X.; Huang, K.-J.; Liu, Y. Novel electrochemical dual-aptamer-based sandwich biosensor using molybdenum disulfide/carbon aerogel composites and Au nanoparticles for signal amplification. *Biosens. Bioelectron.* **2015**, *71*, 171–178. [[CrossRef](#)]
56. Lorenzo-Gómez, R.; Fernández-Alonso, N.; Miranda-Castro, R.; de-los-Santos-Álvarez, N.; Lobo-Castañón, M.J. Unravelling the lipocalin 2 interaction with aptamers: May rolling circle amplification improve their functional affinity? *Talanta* **2019**, *197*, 406–412. [[CrossRef](#)]
57. Aydoğdu Tığ, G.; Pekyardımcı, Ş. An electrochemical sandwich-type aptasensor for determination of lipocalin-2 based on graphene oxide/polymer composite and gold nanoparticles. *Talanta* **2020**, *210*, 120666. [[CrossRef](#)] [[PubMed](#)]
58. Salimi, A.; Khezrian, S.; Hallaj, R.; Vaziry, A. Highly sensitive electrochemical aptasensor for immunoglobulin E detection based on sandwich assay using enzyme-linked aptamer. *Anal. Biochem.* **2014**, *466*, 89–97. [[CrossRef](#)]
59. Eissa, S.; Zourob, M. Aptamer-based label-free electrochemical biosensor array for the detection of total and glycosylated hemoglobin in human whole blood. *Sci. Rep.* **2017**, *7*, 1–8. [[CrossRef](#)] [[PubMed](#)]
60. Díaz-Fernández, A.; Miranda-Castro, R.; de-los-Santos-Álvarez, N.; Rodríguez, E.F.; Lobo-Castañón, M.J. Focusing aptamer selection on the glycan structure of prostate-specific antigen: Toward more specific detection of prostate cancer. *Biosens. Bioelectron.* **2019**, *128*, 83–90. [[CrossRef](#)] [[PubMed](#)]
61. Díaz-Fernández, A.; Miranda-Castro, R.; Díaz, N.; Suárez, D.; de-los-Santos-Álvarez, N.; Lobo-Castañón, M. Aptamers targeting protein-specific glycosylation in tumor markers: General selection, characterization and structural modeling. *Chem. Sci.* **2020**, *11*, 9402–9413. [[CrossRef](#)]
62. Kashfi-Kheyraadi, L.; Mehrgardi, M.A. Aptamer-based electrochemical biosensor for detection of adenosine triphosphate using a nanoporous gold platform. *Bioelectrochemistry* **2013**, *94*, 47–52. [[CrossRef](#)]

63. Sun, D.; Lin, X.; Lu, J.; Wei, P.; Luo, Z.; Lu, X.; Chen, Z.; Zhang, L. DNA nanotetrahedron-assisted electrochemical aptasensor for cardiac troponin I detection based on the co-catalysis of hybrid nanozyme, natural enzyme and artificial DNAzyme. *Biosens. Bioelectron.* **2019**, *142*, 111578. [[CrossRef](#)]
64. Luo, Z.; Sun, D.; Tong, Y.; Zhong, Y.; Chen, Z. DNA nanotetrahedron linked dual-aptamer based voltammetric aptasensor for cardiac troponin I using a magnetic metal-organic framework as a label. *Microchim. Acta* **2019**, *186*, 374. [[CrossRef](#)]
65. Villalongo, A.; Estabiel, I.; Perez-Calabuig, A.M.; Mayol, B.; Parrado, C.; Villalongo, R. Amperometric aptasensor with sandwich-type architecture for troponin I based on carboxyethylsilanetriol-modified graphene oxide coated electrodes. *Biosens. Bioelectron.* **2021**, *183*, 113203. [[CrossRef](#)]
66. Jo, H.; Her, J.; Lee, H.; Shim, Y.-B.; Ban, C. Highly sensitive amperometric detection of cardiac troponin I using sandwich aptamers and screen-printed carbon electrodes. *Talanta* **2017**, *165*, 442–448. [[CrossRef](#)]
67. Ou, D.; Sun, D.; Lin, X.; Liang, Z.; Zhong, Y.; Chen, Z. A dual-aptamer-based biosensor for specific detection of breast cancer biomarker HER2 via flower-like nanozymes and DNA nanostructures. *J. Mat. Chem. B* **2019**, *7*, 3661–3669. [[CrossRef](#)]
68. Jiang, B.; Wang, M.; Chen, Y.; Xie, J.; Xiang, Y. Highly sensitive electrochemical detection of cocaine on graphene/AuNP modified electrode via catalytic redox-recycling amplification. *Biosens. Bioelectron.* **2012**, *32*, 305–308. [[CrossRef](#)]
69. Zhu, X.; Yang, J.; Liu, M.; Wu, Y.; Shen, Z.; Li, G. Sensitive detection of human breast cancer cells based on aptamer–cell–aptamer sandwich architecture. *Anal. Chim. Acta* **2013**, *764*, 59–63. [[CrossRef](#)]
70. Yazdanparast, S.; Benvidi, A.; Banaei, M.; Nikukar, H.; Tezerjani, M.D.; Azimzadeh, M. Dual-aptamer based electrochemical sandwich biosensor for MCF-7 human breast cancer cells using silver nanoparticle labels and a poly(glutamic acid)/MWNT nanocomposite. *Microchim. Acta* **2018**, *185*, 405. [[CrossRef](#)]
71. Abbaspour, A.; Norouz-Sarvestani, F.; Noori, A.; Soltani, N. Aptamer-conjugated silver nanoparticles for electrochemical dual-aptamer-based sandwich detection of staphylococcus aureus. *Biosens. Bioelectron.* **2015**, *68*, 149–155. [[CrossRef](#)]
72. Kim, S.H.; Nam, O.; Jin, E.; Gu, M.B. A new coccolith modified electrode-based biosensor using a cognate pair of aptamers with sandwich-type binding. *Biosens. Bioelectron.* **2019**, *123*, 160–166. [[CrossRef](#)]
73. Liu, Z.; Wang, H. An antifouling interface integrated with HRP-based amplification to achieve a highly sensitive electrochemical aptasensor for lysozyme detection. *Analyst* **2019**, *144*, 5794–5801. [[CrossRef](#)]
74. Diba, F.S.; Kim, S.; Lee, H.J. Amperometric bioaffinity sensing platform for avian influenza virus proteins with aptamer modified gold nanoparticles on carbon chips. *Biosens. Bioelectron.* **2015**, *72*, 355–361. [[CrossRef](#)]
75. Ocaña, C.; Hayat, A.; Mishra, R.; Vasilescu, A.; del Valle, M.; Marty, J.-L. A novel electrochemical aptamer–antibody sandwich assay for lysozyme detection. *Analyst* **2015**, *140*, 4148–4153. [[CrossRef](#)]
76. Lee, S.; Hayati, S.; Kim, S.; Lee, H.J. Determination of protein tyrosine kinase-7 concentration using electrocatalytic reaction and an aptamer-antibody sandwich assay platform. *Catal. Today* **2021**, *359*, 76–82. [[CrossRef](#)]
77. Jung, J.-W.; Shin, W.-S.; Song, J.; Lee, S.-T. Cloning and characterization of the full-length mouse Ptk7 cDNA encoding a defective receptor protein tyrosine kinase. *Gene* **2004**, *328*, 75–84. [[CrossRef](#)]
78. Qureshi, A.; Gurbuz, Y.; Niazi, J.H. Capacitive aptamer–antibody based sandwich assay for the detection of VEGF cancer biomarker in serum. *Sens. Actuators B Chem.* **2015**, *209*, 645–651. [[CrossRef](#)]
79. Zhou, Y.; Zhang, H.; Liu, L.; Li, C.; Chang, Z.; Zhu, X.; Ye, B.; Xu, M. Fabrication of an antibody-aptamer sandwich assay for electrochemical evaluation of levels of  $\beta$ -amyloid oligomers. *Sci. Rep.* **2016**, *6*, 1–8. [[CrossRef](#)]
80. Shui, B.; Tao, D.; Cheng, J.; Mei, Y.; Jaffrezic-Renault, N.; Guo, Z. A novel electrochemical aptamer-antibody sandwich assay for the detection of tau-381 in human serum. *Analyst* **2018**, *143*, 3549–3554. [[CrossRef](#)]
81. Wang, J.; Munir, A.; Li, Z.; Zhou, H.S. Aptamer-Au NPs conjugates-accumulated methylene blue for the sensitive electrochemical immunoassay of protein. *Talanta* **2010**, *81*, 63–67. [[CrossRef](#)] [[PubMed](#)]
82. Wang, J.; Guo, J.; Zhang, J.; Zhang, W.; Zhang, Y. RNA aptamer-based electrochemical aptasensor for C-reactive protein detection using functionalized silica microspheres as immunoprobes. *Biosens. Bioelectron.* **2017**, *95*, 100–105. [[CrossRef](#)] [[PubMed](#)]
83. Centi, S.; Bonel Sanmartin, L.; Tombelli, S.; Palchetti, I.; Mascini, M. Detection of C Reactive Protein (CRP) in Serum by an Electrochemical Aptamer-Based Sandwich Assay. *Electroanal. Int. J. Devoted Fundam. Pract. Asp. Electroanal.* **2009**, *21*, 1309–1315. [[CrossRef](#)]
84. Zhu, G.; Lee, H.J. Electrochemical sandwich-type biosensors for  $\alpha$ -1 antitrypsin with carbon nanotubes and alkaline phosphatase labeled antibody-silver nanoparticles. *Biosens. Bioelectron.* **2017**, *89*, 959–963. [[CrossRef](#)] [[PubMed](#)]
85. Huang, Y.; Nie, X.-M.; Gan, S.-L.; Jiang, J.-H.; Shen, G.-L.; Yu, R.-Q. Electrochemical immunosensor of platelet-derived growth factor with aptamer-primed polymerase amplification. *Anal. Biochem.* **2008**, *382*, 16–22. [[CrossRef](#)] [[PubMed](#)]
86. Taleat, Z.; Cristea, C.; Marrazza, G.; Mazloum-Ardakani, M.; Săndulescu, R. Electrochemical immunoassay based on aptamer–protein interaction and functionalized polymer for cancer biomarker detection. *J. Electroanal. Chem.* **2014**, *717–718*, 119–124. [[CrossRef](#)]
87. Lu, L.; Liu, B.; Leng, J.; Ma, X.; Peng, H. Electrochemical mixed aptamer-antibody sandwich assay for mucin protein 16 detection through hybridization chain reaction amplification. *Anal. Bioanal. Chem.* **2020**, *412*, 7169–7178. [[CrossRef](#)] [[PubMed](#)]
88. Ghalehno, M.H.; Mirzaei, M.; Torkzadeh-Mahani, M. Electrochemical aptasensor for tumor necrosis factor  $\alpha$  using aptamer–antibody sandwich structure and cobalt hexacyanoferrate for signal amplification. *J. Iran. Chem. Soc.* **2019**, *16*, 1783–1791. [[CrossRef](#)]
89. Gu, Y.; Liu, L.; Guo, J.; Xiao, S.; Fang, F.; Yu, X.; Gopinath, S.C.B.; Wu, J.; Liu, X. Biomolecular assembly on interdigitated electrode nanosensor for selective detection of insulin-like growth factor-1. *Art. Cells Nanomed. Biotech.* **2021**, *49*, 30–37. [[CrossRef](#)]
90. You, M.; Yang, S.; An, Y.; Zhang, F.; He, P. A novel electrochemical biosensor with molecularly imprinted polymers and aptamer-based sandwich assay for determining amyloid- $\beta$  oligomer. *J. Electroanal. Chem.* **2020**, *862*, 114017. [[CrossRef](#)]

91. Wang, Q.-L.; Cui, H.-F.; Song, X.; Fan, S.-F.; Chen, L.-L.; Li, M.-M.; Li, Z.-Y. A label-free and lectin-based sandwich aptasensor for detection of carcinoembryonic antigen. *Sens. Actuators B Chem.* **2018**, *260*, 48–54. [[CrossRef](#)]
92. Chai, Y.; Li, X.; Yang, M. Aptamer based determination of the cancer biomarker HER2 by using phosphate-functionalized MnO<sub>2</sub> nanosheets as the electrochemical probe. *Microchim. Acta* **2019**, *186*, 1–6. [[CrossRef](#)]
93. Reily, C.; Stewart, T.J.; Renfrow, M.B.; Novak, J. Glycosylation in health and disease. *Nat. Nephrol.* **2019**, *15*, 346–366. [[CrossRef](#)] [[PubMed](#)]